

Modeling the effects of tropospheric ozone on the growth and yield of global staple crops with DSSAT v4.8.0

Jose Rafael Guarin^{1,2,*}, Jonas Jägermeyr^{1,2}, Elizabeth A. Ainsworth³, Fabio A. A. Oliveira⁴, Senthold Asseng⁵, Kenneth Boote⁴, Joshua Elliott⁶, Lisa Emberson⁷, Ian Foster⁸, Gerrit Hoogenboom⁴, David Kelly⁸, Alex C. Ruane², Katrina Sharps⁹

¹Center for Climate Systems Research, Columbia Climate School, Columbia University, New York, NY 10025 USA

²NASA Goddard Institute for Space Studies, New York, NY 10025 USA

³Global Change and Photosynthesis Research Unit, United States Department of Agriculture, Agricultural Research Service, Urbana, IL 61801

⁴Department of Agricultural and Biological Engineering, University of Florida, Gainesville, FL 32611 USA

⁵School of Life Sciences, HEF World Agricultural Systems Center, Technical University of Munich, Freising, 85354 Germany

⁶Center for Robust Decision-making on Climate and Energy Policy (RDCEP), University of Chicago, Chicago, IL 60637 USA

⁷Environment & Geography Dept., University of York, York, YO10 5NG UK

⁸Department of Computer Science, University of Chicago, Chicago, IL 60637 USA

⁹UK Centre for Ecology & Hydrology, Environment Centre Wales, Bangor, LL57 2UW, UK

*Correspondence to: Jose Rafael Guarin (j.guarin@columbia.edu)

Highlights

- Effects of O₃ stress on photosynthesis and leaf senescence were added to the DSSAT/pDSSAT maize, rice, soybean, and wheat crop models.
- The modified models reproduced growth and yields under different O₃ levels observed in field experiments and reported in the literature.
- Expected detrimental interactions between O₃, CO₂, and water deficit were reproduced with the new models.
- The updated crop models can be used to simulate impacts of O₃ stress under future climate change and air pollution scenarios.

Abstract. Elevated surface ozone (O₃) concentrations can negatively impact growth and development of crop production by reducing photosynthesis and accelerating leaf senescence. Under unabated climate change, future global O₃ concentrations are expected to increase in many regions, adding additional challenges to global agricultural production. Presently, few global process-based crop models consider the effects of O₃ stress on crop growth. Here, we incorporated the effects of O₃ stress on photosynthesis and leaf senescence into the Decision Support System for Agrotechnology Transfer (DSSAT) crop models for maize, rice, soybean, and wheat. The advanced models reproduced the reported yield declines from observed O₃-dose field experiments and O₃ exposure responses reported in the literature (O₃ relative yield loss RMSE < 10% across all calibrated models). Simulated crop yields decreased as daily O₃ concentrations increased above 25 ppb, with average yield losses of 0.16% to 0.82% (maize), 0.05% to 0.63% (rice), 0.36% to 0.96% (soybean), and 0.26% to 1.23% (wheat) per ppb O₃ increase, depending on the cultivar O₃ sensitivity. Increased water deficit stress and elevated CO₂ lessen the negative impact of elevated O₃ on crop yield,

but potential yield gains from CO₂ concentration increases may be counteracted by higher O₃ concentrations in the future, a potentially important constraint to global change projections for the latest process-based crop models. The improved DSSAT models with O₃ representation simulate the effects of O₃ stress on crop growth and yield in interaction with other growth factors and can be run in the parallel DSSAT global gridded modeling framework for future studies on O₃ impacts under climate change and air pollution scenarios across agroecosystems globally.

Keywords

Surface ozone, climate change, global process-based crop model, phytotoxicity, staple crop yield

1 Introduction

Surface or ground-level, ozone (O₃) is a major air pollutant that causes adverse impacts on agricultural productivity worldwide (Mills et al., 2018b; Emberson et al., 2018; Tai et al., 2021). O₃ is formed through photochemical reactions between incoming solar radiation and primary pollutants such as Nitrogen Oxides (NO_x = NO + NO₂), Volatile Organic Compounds (VOCs), Carbon Monoxide (CO), or Methane (CH₄) across all areas of the globe (Cooper et al., 2014; Simpson et al., 2014). Global O₃ concentrations have increased 2-7% per decade in northern mid-latitude regions and 2-12% per decade in tropical regions since the mid-1990s (Ipcc, 2021; Arias et al., 2021). Future O₃ concentrations are projected to continue increasing if O₃ precursor emissions are not mitigated, i.e., following the shared socio-economic pathways where regional rivalry leads to doubling of CO₂ emissions by 2100 (SSP3-7.0) or where fossil fuel enabled growth leads to doubling of CO₂ emissions by 2050 (SSP5-8.5) (Ipcc, 2021; Arias et al., 2021; Szopa et al., 2021; Griffiths et al., 2021).

Crops exposed to elevated levels of O₃ concentrations can experience reduced photosynthesis, accelerated senescence, foliar chlorosis and even necrosis from increased cumulative oxidative stress (Ainsworth, 2017). These negative effects lead to decreased productivity resulting in global yield losses between 2-16% for the four main staple crops: maize, rice, soybean, and wheat (Ainsworth, 2017; Schiferl and Heald, 2018; Emberson, 2020), with global annual economic damages of approximately \$34 billion (Sampedro et al., 2020; Feng et al., 2022). Climate change may exacerbate the negative effects from elevated O₃ concentrations because O₃ concentrations are highest in summer months and the projected higher temperatures with more frequent heat waves may lead to a longer period of more active photochemical reactions (Zhang and Wang, 2016; Hou and Wu, 2016; Szopa et al., 2021). Elevated concentrations of atmospheric CO₂ and increased periods of water deficit stress cause stomatal closure that can reduce crop O₃ uptake (Khan and Soja, 2003; Biswas et al., 2013), but in turn potential yield gains associated with the CO₂ fertilization effect (Toreti et al., 2020; Jagermeyr et al., 2021) may be constrained by elevated O₃. Therefore, it is important to evaluate net O₃ effects for crop growth and consider the effects of O₃ in global agricultural assessments examining future scenarios.

Process-based crop simulation models have been used to evaluate the impacts of O₃ on crop yields (Guarin et al., 2019; Tai et al., 2021), but most global gridded process-based crop models are still unable to respond to O₃ stress. Recently, the global Lund-Potsdam-Jena managed Land (LPJmL) and Joint UK Land Environment Simulator

(JULES) models were modified to include the effects of O₃ stress on soybean and wheat growth (Schauberger et al., 2019; Leung et al., 2020). Additionally, the Agricultural Model Intercomparison and Improvement Project (AgMIP; Rosenzweig et al. (2013)) Ozone Team has recently developed protocols for incorporating O₃ stress into a wider body of crop models aiming to establish the first multi-model assessment of ozone impacts in agriculture at global level (Emberson et al., 2018).

The aim of this study is to incorporate the effects of O₃ concentrations into the stress response functions of the maize, rice, soybean, and wheat models within the established Decision Support System for Agrotechnology Transfer (DSSAT) v4.8.0 modeling platform (Jones et al., 2003; Hoogenboom et al., 2019), and consequently the parallel DSSAT (pDSSAT) v4.8.0 global gridded modeling platform that is used to run DSSAT in a global setup (Elliott et al., 2014), to simulate O₃ effects on global crop development and yield for the four major staple crops. The observational data from the Free-air CO₂ Enrichment (FACE) field experiments conducted in Champaign, Illinois, USA (Choquette et al., 2020; Betzelberger et al., 2012) and well-known O₃ exposure relationships reported in the literature are used to develop and calibrate the model O₃ response functions. Additionally, the observed interactions between O₃, CO₂, and water deficit stress are examined via sensitivity analyses conducted with the modified models.

2 Materials and Methods

2.1 Description of crop models

The crop models within the pDSSAT parallel modeling environment are based on the existing crop models within the widely used DSSAT crop modeling platform (Jones et al., 2003; Hoogenboom et al., 2019) combined with the Center for Robust-Decision Making on Climate and Energy Policy (RDCEP) Parallel System for Integrating Impact Models and Sectors (pSIMS) framework (Elliott et al., 2014) to allow for global gridded process-based crop modeling on high performance computational systems. The O₃ stress routines presented here are also applied in the standard DSSAT crop models and can be used for field level simulations and point-based testing in addition to the global-level modeling applications.

The four DSSAT crop models used in this study are the Crop Environment Resource Synthesis (CERES) -Maize, CERES-Rice, Crop Growth Simulation (CROPGRO) -Soybean, and Nitrogen Wheat (NWheat) models that have been used in previous AgMIP crop model intercomparisons (Bassu et al., 2014; Li et al., 2015; Asseng et al., 2015; Kothari et al., 2022). The CERES-Maize and CERES-Rice models were previously used to estimate global ozone crop losses (Schiferl and Heald, 2018); however, their approach was based on the multiplication of the simulated global base production by the relative yield-O₃ response functions to determine a response proxy. The approach used in this present study integrates daily process-based stress calculations to simulate daily crop growth and stress dynamics. Thus, the models are more applicable to a much broader range of scenarios given that they can combine daily stress interactions and can be used to scale across agroecosystems in a more robust way.

2.2 O₃ incorporation into the crop models

105 The incorporation of O₃ effects into the DSSAT crop models followed the same methodology as the O₃ incorporation
 into the DSSAT-NWheat crop model (Guarin et al., 2019), which was based on the incorporation of previous abiotic
 stress routines (Asseng et al., 2004). O₃ response was added to the models via the inclusion of daily photosynthesis
 reduction and leaf senescence acceleration functions. Additionally, the interaction between O₃ and water deficit stress
 and/or atmospheric CO₂ concentrations was incorporated into the models since these combined interactions can
 110 mitigate impacts from O₃ on crop production and vice-versa. For example, water deficit stress that induces stomatal
 closure in turn limits O₃ stress because of reduced aerosol uptake (Khan and Soja, 2003; Biswas et al., 2013).

2.2.1 CERES-Maize and CERES-Rice models

The effects of O₃ were incorporated into the CERES-Maize and CERES-Rice models using similar methodology since
 these two models share similar code. O₃ was added into the models using a photosynthesis reduction stress factor
 115 (FO₃) following Eq. (1):

$$FO_3 = \max\left(0.0, -\left(\frac{FOZ_1}{100}\right) * OZON_7 + \left(1.0 + \left(\frac{FOZ_1}{100}\right) * 25.0\right)\right), \quad (1)$$

where OZON₇ is the daily mean 7-hour (M7, 9:00 – 15:59 hr) O₃ concentration (ppb) and FOZ₁ is the O₃ stress
 parameter for photosynthesis calibrated for different O₃ sensitivities of cultivars divided by a decimal correction factor
 of 100. The decimal correction factor ensures that the FOZ₁ parameter value ranges between 0.0 and 1.0 in the model
 120 ecotype parameter file for comprehensible user input. A minimum M7 O₃ threshold of 25 ppb was set as the reference
 value based on pre-industrial O₃ concentrations and the United States National Crop Loss Assessment Network
 (NCLAN) studies indicating that O₃ damage within crops occurs above this threshold (Heck et al., 1984; Lesser et al.,
 1990; Feng and Kobayashi, 2009). When the daily M7 O₃ concentration exceeds this threshold, photosynthesis is
 reduced by a factor between 0.0 to 1.0 (Eq. (1)) and leaf senescence is accelerated by a factor between 0.0 to 1.0 (Eq.
 125 (5)). The M7 O₃ metric was chosen as the model input because it is the most readily available metric in the literature,
 and conversion functions exist to convert between M7 and AOT40, daily mean 12-hour (M12), or daily mean 24-hour
 (M24) O₃ metrics (Osborne et al., 2016).

Eq. (1) does not include the interaction of O₃ stress with water deficit stress or elevated atmospheric CO₂. To consider
 these combined interactions on crop growth (PRFO₃), FO₃ was modified using Eq. (2):

$$130 \quad PRFO_3 = \min\left(1.0, \left(\frac{FO_3 * PCO_2}{SWFAC}\right)\right), \quad (2)$$

where PCO₂ is the atmospheric CO₂ effect on potential daily dry matter production and SWFAC is the water stress
 factor on photosynthesis (Jones and Kiniry, 1986; Ritchie et al., 1987; Jones et al., 2003). Since PCO₂ is always greater
 than one, multiplying by the CO₂ effect mitigates the reduction caused by FO₃. Because SWFAC is a reduction factor
 between zero and one, dividing by this factor decreases the reduction from FO₃ under increased water deficit stress
 135 conditions.

The simulated daily biomass production (CARBO, g plant⁻¹ day⁻¹) within the models was calculated based on the
 existing photosynthesis stress factors with the addition of PRFO₃ using Eq. (3) for maize and Eq. (4) for rice:

$$CARBO_{maize} = PCARB * \min(PRFT, SWFAC, NSTRES, PSTRES_1, KSTRES, PRFO_3) * SLPF, \quad (3)$$

$$CARBO_{rice} = PCARB * \min(PRFT, SWFAC, NSTRES, TSHOCK, PSTRES_1, KSTRES, PRFO_3) * SLPF, \quad (4)$$

140 where PCARB is daily potential dry matter production of the crop accounting for light interception, radiation use efficiency, and the CO₂ effect on photosynthesis (g plant⁻¹), PRFT, SWFAC, NSTRES, TSHOCK (CERES-Rice only), PSTRES₁, KSTRES, and PRFO₃ are the temperature, soil water, Nitrogen, transplanting shock, Phosphorous, Potassium, and O₃ stress factors on photosynthesis, respectively, and SLPF is the soil fertility factor (Jones and Kiniry, 1986; Ritchie et al., 1987; Jones et al., 2003).

145

Leaf senescence acceleration due to O₃ stress (SLFO₃) was added to the models using Eq. (5):

$$SLFO_3 = \max\left(0.0, -\left(\frac{SFOZ_1}{1000}\right) * OZON_7 + \left(1.0 + \left(\frac{SFOZ_1}{1000}\right) * 25.0\right)\right), \quad (5)$$

150

where SFOZ₁ is the O₃ stress parameter for leaf senescence calibrated for different O₃ sensitivities of cultivars divided by a decimal correction factor of 1000 (to ensure the SFOZ₁ parameter value ranges between 0.0 and 1.0 in the model ecotype file). The SLFO₃ factor was then included in the existing daily rate of leaf area senescence function (PLAS, cm² day⁻¹) within the models as shown in Eq. (6) for maize and Eq. (7) for rice:

$$PLAS_{maize} = (PLA - SENLA) * \left(1 - \min(SLFW, SLFC, SLFT, SLFN, SLFP, SLFO_3)\right), \quad (6)$$

$$PLAS_{rice} = (PLA - SENLA) * \left(1 - \min(SLFW, SLFC, SLFT, SLFN, SLFP, SLFK, SLFO_3)\right), \quad (7)$$

155

where PLA is daily plant leaf area (cm² plant⁻¹), SENLA is daily normal leaf senescence (cm² plant⁻¹), and SLFW, SLFC, SLFT, SLFN, SLFP, SLFK, and SLFO₃ are the leaf senescence stress factors due to water, light competition, temperature, Nitrogen, Phosphorous, Potassium (CERES-Rice only), and O₃ stress, respectively (Jones and Kiniry, 1986; Ritchie et al., 1987; Jones et al., 2003).

2.2.2 CROPGRO-Soybean model

160

The effects of O₃ were incorporated into the CROPGRO-Soybean model using a similar approach as described in the CERES crop models. O₃ was added into the model using the same FO₃ and PRFO₃ factors as in Eq. (1) and Eq. (2) (for Eq. (2), PCO₂ is called PRATIO in CROPGRO-Soybean). However, CROPGRO-Soybean calculates daily photosynthesis differently than the other models and has two different photosynthesis calculation options, leaf or canopy photosynthesis (Wilkerson et al., 1983; Boote and Pickering, 1994; Jones et al., 2003). This study focuses on the default leaf photosynthesis calculation option (which was modified to read in the CO₂ ratio effect for the PRFO₃ interaction). The daily gross photosynthesis (PG, g [CH₂O] m⁻² day⁻¹) within the model was calculated based on the limiting photosynthesis stress factors using Eq. (8) for leaf photosynthesis and Eq. (9) for canopy photosynthesis:

165

$$PG_{leaf} = \left(\frac{PGDAY}{44.0} * 30.0 * SLPF\right) * \min(SWFAC, PRFO_3) * PSTRES_1, \quad (8)$$

$$PG_{canopy} = PTSMAX * SLPF * PG_{FAC} * TPG_{FAC} * E_{FAC} * PGSLW * PRATIO * PGLFMX * \min(SWFAC, PRFO_3), \quad (9)$$

170 where PGDAY is daily potential photosynthesis ($\text{g} [\text{CH}_2\text{O}] \text{m}^{-2} \text{day}^{-1}$), SWFAC, PSTRES₁, and PRFO₃ are the soil
 water, Phosphorous, and O₃ stress factors on photosynthesis, respectively. PTSMAX is the potential amount of CH₂O
 that can be produced for the full canopy ($\text{g} [\text{CH}_2\text{O}] \text{m}^{-2} \text{day}^{-1}$), PG_{FAC} is a factor to compute daily PG as a function of
 leaf area index, TPG_{FAC} is a reduction factor due to less than optimal daytime temperature, E_{FAC} is the effect of
 Nitrogen and Phosphorous stress on daily canopy photosynthesis, PGSLW is the relative effect of leaf thickness on
 175 daily canopy photosynthesis, and PRATIO is the relative effect of atmospheric CO₂ on daily canopy photosynthesis
 (Boote and Pickering, 1994).

Leaf senescence acceleration due to O₃ stress (SLFO₃) was added to CROPGRO-Soybean using Eq. (10):

$$SLFO_3 = \max\left(0.0, \left(\frac{SFOZ_1}{1000}\right) * OZON_7 - \left(\left(\frac{SFOZ_1}{1000}\right) * 25.0\right) * WTLF\right), \quad (10)$$

180 where WTLF is the dry mass of leaf tissue ($\text{g}_{\text{leaf}} \text{m}^{-2}$). The CROPGRO leaf senescence routine is based on existing
 WTLF using a different approach than the CERES leaf senescence reduction factor, so SLFO₃ has the opposite trend
 when compared to the CERES model calculation (Fig. 1). The SLFO₃ factor was then included in the existing daily
 defoliation due to daily leaf senescence (SLDOT, $\text{g} \text{m}^{-2} \text{day}^{-1}$) calculation within the model as shown in Eq. (11):

$$SLDOT = SLDOT_n + \max(SLNDOT, SLFO_3), \quad (11)$$

where SLDOT_n is the natural daily leaf senescence and SLNDOT and SLFO₃ are the daily leaf senescence due to
 water and O₃ stress ($\text{g} \text{m}^{-2} \text{day}^{-1}$), respectively.

185 2.2.3 DSSAT-NWheat model

The incorporation of O₃ into the NWheat crop model was described and validated in Guarin et al., (2019) and was
 used as the reference for the maize, rice, and soybean models. The approach used the same FO₃ and PRFO₃ equations
 as in Eq. (1) and (2) (note that the NWheat equations were simplified from Guarin et al., (2019) by the decimal
 correction factor and single FOZ₁ parameter as in Eq. (1) for consistency among all models) and a similar SLFO₃
 190 shown in Eq. (12):

$$SLFO_3 = \left(\frac{SFOZ_1}{10}\right) * OZON_7 + \left(1.0 - \left(\frac{SFOZ_1}{10} * 25.0\right)\right). \quad (12)$$

The O₃ effect for the different cultivar sensitivities is controlled by the FOZ₁ and SFOZ₁ parameters, as in the other
 models (the SFOZ₁ parameter is divided by 10 to ensure that the value ranges between 0.0 and 1.0 in the model ecotype
 file). The decimal correction factors vary between the crop models because the different models calculate stresses
 using different magnitudes.
 195

The FO₃ and SLFO₃ responses calculated over increasing M7 O₃ concentrations are illustrated for each model in Fig.
 1 using the parameter values for different O₃ cultivar classifications shown in Table 1. The FOZ₁ and SFOZ₁ parameter
 values for all models were determined from the cultivar sensitivities observed in the field experiments (section 2.3)
 and the sensitivities derived from the O₃ exposure relationships from the literature (section 2.5).

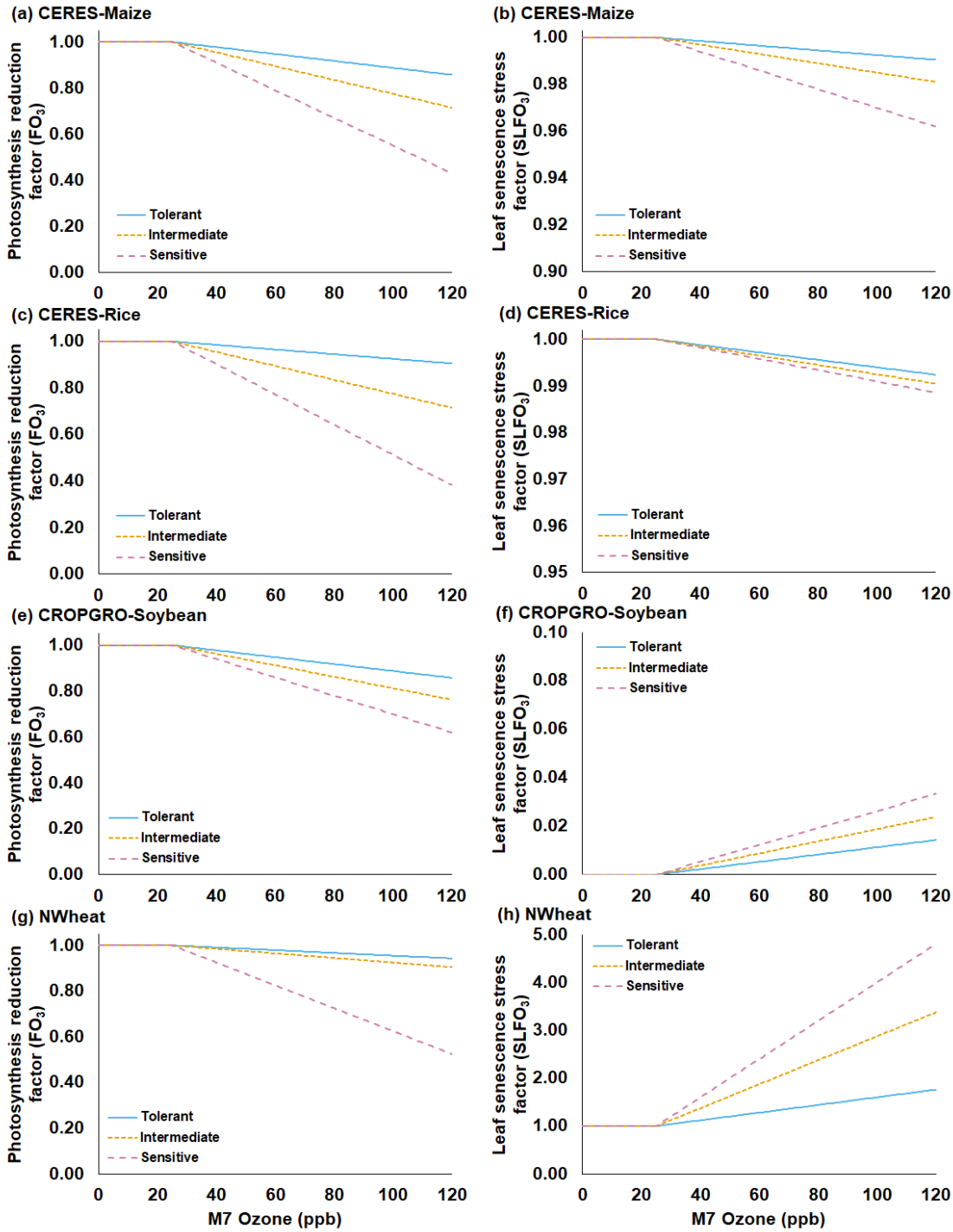


Figure 1: Functions for the O_3 photosynthesis reduction factor without interaction of water deficit stress and CO_2 fertilization effect (FO_3) (first column) and the O_3 leaf senescence acceleration stress factor ($SLFO_3$) (second column) under increasing mean 7-hour ($M7$) O_3 concentrations for the (a, b) CERES-Maize, (c, d) CERES-Rice, (e, f) CROPGRO-Soybean, and (g, h) NWheat models. Each figure shows three different O_3 sensitivity cultivar classifications derived from the O_3 exposure-yield responses from the literature: tolerant (blue solid line), intermediate (gold short-dash line), and sensitive (magenta long-dash line). $SLFO_3$ for CROPGRO-Soybean (Eq. (10)) shown with leaf tissue dry mass ($WTLF$) of 1 g m^{-2} for simplicity. Steeper slopes indicate a higher sensitivity to O_3 for both FO_3 and $SLFO_3$. Table 1 shows the parameters used in the equations for each classification of O_3 sensitivity (Eq. (1), (5), (10), and (12)).

205

210

Table 1: Summary of the O₃ photosynthesis stress parameters (FOZ₁) and the O₃ leaf senescence stress parameters (SFOZ₁) used in the FO₃ and SLFO₃ calculations (Eq. (1), (5), (10), and (12)) for the four DSSAT models under three different O₃ sensitivity cultivar classifications. The CERES and CROPGRO parameter values were determined from the O₃ exposure-yield responses in the literature (Fig. S2, Fig. S3). NWheat parameter values were from Guarin et al., (2019) and confirmed with the literature.

| O ₃ sensitivity cultivar classifications | CERES-Maize | | CERES-Rice | | CROPGRO-Soybean | | NWheat | |
|---|------------------|-------------------|------------------|-------------------|------------------|-------------------|------------------|-------------------|
| | FOZ ₁ | SFOZ ₁ | FOZ ₁ | SFOZ ₁ | FOZ ₁ | SFOZ ₁ | FOZ ₁ | SFOZ ₁ |
| Tolerant | 0.15 | 0.10 | 0.10 | 0.08 | 0.15 | 0.15 | 0.06 | 0.08 |
| Intermediate | 0.30 | 0.20 | 0.30 | 0.10 | 0.25 | 0.25 | 0.10 | 0.25 |
| Sensitive | 0.60 | 0.40 | 0.65 | 0.12 | 0.40 | 0.35 | 0.50 | 0.40 |

2.3 Observed O₃ exposure field experiments

In general, detailed field experiments of crop growth under elevated O₃ conditions for different crops are scarce and limit the granularity of model calibration. All field experiments examined in this study used dominant management conditions to limit other stresses besides O₃, e.g., water deficit or N stress, so the simulations assumed negligible outside stresses. For each crop, the DSSAT phenological and growth parameters were calibrated based on the observed control treatment with minimal O₃ stress to ensure that the models were functioning properly regardless of O₃ impact. Then, the O₃ response parameters, FOZ₁ and SFOZ₁, were calibrated based on the observed O₃ exposure-yield response between the elevated O₃ treatments and the control to simulate the O₃ effect.

For maize, the FACE experiment conducted at Champaign, Illinois, USA (40.03 °N, 88.27 °W, 230 m elevation) in 2018 was used for calibrating the CERES-Maize model (Choquette et al., 2020). The maize FACE experiment consisted of six cultivars grown under an ambient and an elevated O₃ treatment with $n = 4$ (Table 2). Since there was only one year of data, the model was validated against the O₃ exposure-relative yield response functions from the literature (section 2.5). The daily maximum temperature (TMAX), minimum temperature (TMIN), and precipitation (RAIN) weather data were collected from the nearby National Oceanic and Atmospheric Administration (NOAA) Willard airport weather station and the daily incoming solar radiation (SRAD) was collected from the National Aeronautics and Space Administration (NASA) Prediction Of Worldwide Energy Resources (POWER) database (<https://power.larc.nasa.gov/>). The soil consisted of the Drummer silty clay loam soil series, and the soil parameters for this series were obtained from the United States Department of Agriculture (USDA) Natural Resources Conservation Service (NRCS) Web Soil Survey database (Table S1) (NRCS, 2023). The cultivars were planted in two 3.5 m rows with a row spacing of 0.76 m on May 13, 2018 (Choquette et al., 2020). The hourly O₃ fumigation (from 10:00 to 18:00) began on May 25, 2018 and ended on August 14, 2018 and was used to calculate the daily M7 O₃ concentrations. The cultivar plots were harvested at maturity on September 21, 2018. N and water deficit stress were reported to be non-limiting, so the simulations used the non-limiting N setting within the model and the simulated water stress was confirmed to be non-limiting with the provided rainfall. The DSSAT cultivar parameters were calibrated for phenology and growth under negligible stress conditions using the treatment with the ambient O₃ concentration (38 ppb) for each cultivar. After the phenology and growth cultivar parameters were calibrated, the FOZ₁ and SFOZ₁ O₃ response parameters were calibrated using the yield response from the elevated O₃ concentration treatments (Fig. S1 (a)).

245 For soybean, data from the FACE experiment conducted at the same location in Champaign, Illinois, USA (40.03 °N, 88.27 °W, 230 m elevation) in 2009 and 2010 was used for model testing (Betzberger et al., 2012). The 2009 data was used for model calibration and the 2010 data was used for model validation. These data were previously used to incorporate O₃ effects on leaf photosynthesis into the JULES model (Leung et al., 2020). The SoyFACE experiment consisted of seven soybean cultivars grown under nine O₃ treatments with different target concentrations (Table 2).

250 The hourly O₃ fumigation data (plots fumigated for 8 to 9 hours daily except when leaves were wet) for each treatment was recorded in situ and was used to calculate the daily M7 O₃ concentrations (Betzberger et al., 2012). The weather data was collected from the same sources as used in the maize experiment (NOAA and NASA POWER), and the soil consisted of either the Drummer silty clay loam or the Flanagan silt loam series which were obtained from the USDA NRCS Web Soil Survey database (Table S1). The initial soil conditions of the simulations were set at 95% available

255 water content and 100 kg N ha⁻¹ to minimize water and N stress. The cultivars were planted in plots eight rows wide and 5.4 m long, with a row spacing of 0.38 m, on June 9, 2009 and May 27, 2010. The O₃ fumigation started on June 29, 2009 and June 6, 2010, and ended on September 27, 2009 and September 17, 2010. The cultivar plots were harvested at maturity on October 20, 2009 and September 30, 2010. For each specified cultivar maturity group (Betzberger et al., 2012), the corresponding default DSSAT maturity group parameters were used as reference and

260 then calibrated for phenology and growth under negligible stress using the treatment with the ambient O₃ concentration (37 ppb). After the phenology and growth cultivar parameters were calibrated, the FOZ₁ and SFOZ₁ O₃ response parameters were calibrated using the yield response from the elevated O₃ concentration treatments (Fig. S1 (b)). The parameters for both maize and soybean were calibrated using the one-factor-at-a-time method (Morris, 1991) until the best fit was found for the phenology, aboveground biomass and yield, and relative yield loss for each

265 cultivar across all O₃ treatments.

Table 2: O₃ fumigation target concentration and average mean 7-hour (M7, 9:00 – 15:59 hr) O₃ concentrations for the 2018 maize FACE experiment (Choquette et al., 2020) and the 2009 and 2010 soybean SoyFACE experiments (Betzberger et al., 2012).

| Crop experiment | O ₃ fumigation target concentration (ppb) | Average M7 O ₃ concentration (ppb) |
|-----------------|--|---|
| Maize 2018 | Ambient | 38 |
| | 100 | 77 |
| Soybean 2009 | Ambient | 37 |
| | 40 | 39 |
| | 55 | 47 |
| | 70 | 57 |
| | 85 | 61 |
| | 110 | 75 |
| | 130 | 96 |
| | 160 | 102 |
| | 200 | 126 |
| Soybean 2010 | Ambient | 37 |
| | 55 | 46 |
| | 70 | 52 |
| | 85 | 59 |
| | 110 | 69 |

| | |
|-----|----|
| 130 | 76 |
| 150 | 70 |
| 170 | 84 |
| 190 | 84 |

270

For rice, there was no O₃ field experiment data readily available, thus a representative rice-producing location in the main North American rice-producing area at Stuttgart, Arkansas, USA (34.50 °N, 91.55 °W, 60 m elevation) (USDA NASS, 2010) was simulated with the default DSSAT North American rice cultivar. 2009 was selected for consistency with the soybean simulations. The weather data was collected from the NASA POWER database and the dominant soil series for Arkansas County, Dewitt silt loam, was determined from the USDA NRCS Web Soil Survey database (Table S1) (NRCS, 2023). The initial soil conditions of the simulations were set at 100% available water content and 100 kg N ha⁻¹ to ensure negligible water and N stress. Four 50 kg N ha⁻¹ fertilizer applications were applied throughout the season to ensure negligible N stress in the simulations. The cultivar was planted on April 20, 2009 based on the most active planting dates recorded for Arkansas in the USDA Field Crops handbook (USDA NASS, 2010), and the harvest date was automatically calculated based on when the model simulations reached physiological maturity. The default DSSAT North American rice cultivar parameters were used, and the FOZ₁ and SFOZ₁ O₃ response parameters were calibrated using the yield response from the elevated O₃ exposure functions from the literature (section 2.5).

275

280

For wheat, the NWheat model was calibrated and validated using an air exclusion system O₃ exposure wheat field experiment conducted in Wake County, North Carolina, USA (35.73 °N, 78.68 °W, 116 m elevation) and is described in detail in Guarin et al., (2019).

285

2.4 Sensitivity analysis of O₃ equations and parameters

A sensitivity analysis for maize, rice, and soybean was conducted using simulations of nine constant daily M7 O₃ concentrations of 25, 40, 50, 60, 70, 80, 90, 100, and 120 ppb with different FOZ₁ and SFOZ₁ parameter values under combinations between normal or 50% reduced rainfall and 350 ppm or 550 ppm CO₂ concentrations to confirm that the O₃ modifications and stress interactions within the models were behaving as expected. The simulated locations and management setup for each crop were the same as the field experiments described above (section 2.3). For wheat, the sensitivity analysis was based on the 1993 FACE experiment conducted in Maricopa, Arizona (33.06 °N, 111.98 °W, 361 m elevation) (Hunsaker et al., 1996; Kimball et al., 1999; Kimball et al., 2017). The simulation setup for the Maricopa FACE experiment used the same 9 M7 O₃ concentrations with either a “Wet” irrigation schedule (total of 629 mm sub-surface drip irrigation at 0.23 m from planting to harvest) or a “Dry” irrigation schedule (total of 347 mm sub-surface drip irrigation at 0.23 m from planting to harvest) under 350 ppm and 550 ppm CO₂ concentrations to examine the O₃-CO₂-water interactions as detailed in Guarin et al., (2019). For all crops, each O₃ parameter was first tested independently to examine the individual effects on photosynthesis and leaf senescence, i.e., when examining FOZ₁, SFOZ₁ was set to zero and vice versa.

290

295

300

2.5 Observed O₃ exposure relationships based on the literature

To confirm that the models were able to reproduce the observed relative yield loss due to O₃ stress, the simulated results were compared to well-known literature reports of O₃ exposure metrics and yield response for each crop using the M7 O₃ concentrations. The simulated locations and management conditions were the same experimental conditions as described above for each crop. For each crop, different O₃ classification of cultivar sensitivities were defined based on more severe response to O₃ stress, i.e., tolerant, intermediate, and sensitive. These classifications of cultivar O₃ sensitivity were determined using the extensive literature review data from Mills et al. (2018a) combined with the maize and soybean FACE data for a total of 9 maize cultivars, 50 rice cultivars, 49 soybean cultivars, and 23 wheat cultivars. The literature review consisted of O₃ exposure experiments conducted in open-top chambers, experimental fields, or greenhouses and included the experiments that contributed to the widely applied Weibull O₃ response function (Heck et al., 1984; Adams et al., 1989; Lesser et al., 1990; Wang and Mauzerall, 2004; Tai et al., 2021; Feng et al., 2022). The selection criteria of the data are described in detail in Mills et al. (2018a).

The yield data from the literature experiments were standardized as performed by Mills et al. (2018a) and described by Osborne et al. (2016). For each experiment, linear regression was used to determine the yield at 25 ppb M7 O₃ and this value was the reference for calculating the relative yield, i.e., relative yield was calculated as the actual observed yield divided by the yield at 25 ppb O₃. The 25 ppb M7 O₃ threshold was chosen for proper comparison to the model results. After calculating the yield relative to 25 ppb M7 O₃, a linear regression for each cultivar was performed using R statistical software, v4.3.0, (R Core Team, 2023; Wickham, 2016; Wickham et al., 2023) to determine the O₃ exposure response (Fig. S2). The cultivar O₃ exposure responses were then classified into three evenly distributed quantiles, 0%-33%, 33%-66%, and 66%-100%, chosen to represent the three O₃ sensitivity classifications: sensitive, intermediate, and tolerant, respectively (Fig. S3). These data were used to determine the model FOZ₁ and SFOZ₁ values of each of the O₃ cultivar classifications shown in Table 1 to evaluate if the models could accurately reproduce the O₃ exposure-yield responses.

3 Results

3.1 Calibration of crop models and simulated relative yield loss against O₃ exposure field experiments

The simulated phenology (anthesis [flowering] and physiological maturity dates), biomass, yield, and relative yield due to elevated O₃ stress from the maize and soybean experiments were compared to the field observations to determine performance of the O₃ equations within the models (Tables 3 – 5, Fig. 2 and 3, Fig. S1). The relative yield due to O₃ stress was calculated by dividing the yield of each corresponding O₃ treatment over the control yield, i.e., the baseline O₃ treatment, and multiplying by 100 to convert to a percentage. The relative yield loss was the difference between 100% and the calculated relative yield. There was no O₃ field experiment data for rice, so the rice O₃ parameter values and performance were compared to the O₃ exposure-yield response functions from the literature (section 3.3).

The maize and soybean cultivars had different sensitivities to O₃ stress which were accounted for by using different FOZ₁ and SFOZ₁ values (Fig. S1). The calibrated CERES-Maize and CROPGRO-Soybean models simulated the physiological maturity within four days of the observations (Table 5; Root Mean Square Error (RMSE) = 0.0 days for

maize 2018, 3.70 days for soybean 2009, and 3.30 days for soybean 2010). The calibrated CERES-Maize model was able to reproduce the yield and relative yield loss very well across all six cultivars (Fig. 2; RMSE = 107 kg ha⁻¹ and 2%; r² = 0.99 and 0.99, respectively). This ideal model performance was because only two O₃ treatments were available for each maize cultivar which simplified the calibration process (Fig. S1 (a)). The CROPGRO-Soybean model was able to reproduce the biomass, yield, and relative yield loss due to O₃ stress well for the calibration year, 2009 (Fig. 3 (a), (b), (c); RMSE = 1179 kg ha⁻¹, 328 kg ha⁻¹, and 10%; r² = 0.81, 0.88, and 0.85), and acceptably for the evaluation year, 2010, across all seven cultivars (Fig. 3 (d), (e), (f); RMSE = 3339 kg ha⁻¹, 1291 kg ha⁻¹, and 16%; r² = 0.59, 0.71, and 0.66). The model overestimated biomass and yield for all cultivars and treatments in 2010, which was likely the result of a factor outside of the model setup that mitigated the increased incoming solar radiation when compared to 2009 (section 4.3). The calibration and evaluation for the NWheat model was conducted and validated in Guarin et al. (2019), where the model reproduced the observed relative yield due to O₃ stress with a Normalized Root Mean Square Error (NRMSE) of 23% and an r² of 0.94, 0.91, and 0.88 for the tolerant, intermediate, and sensitive O₃ sensitive cultivar classifications.

Table 3: CERES-Maize cultivar and O₃ parameters used to simulate the six maize cultivars from the 2018 FACE field experiment (Choquette et al., 2020). P1 = Thermal time from seedling emergence to the end of the juvenile phase (expressed in degree days above a base temperature of 8 °C), P2 = Extent to which daily development is delayed for each hour increase in photoperiod above the longest photoperiod at which development proceeds at a maximum rate (which is considered to be 12.5 hours), P5 = Thermal time from silking to physiological maturity (expressed in degree days above a base temperature of 8 °C), G2 = Maximum possible number of kernels per plant, G3 = Kernel filling rate during the linear grain filling stage and under optimum conditions (mg day⁻¹), PHINT = Phylochron interval, i.e., the interval in thermal time (degree days) between successive leaf tip appearances, FOZ₁ = O₃ effect on photosynthesis, and SFOZ₁ = O₃ effect on leaf senescence.

| Cultivar | P1 | P2 | P5 | G2 | G3 | PHINT | FOZ ₁ | SFOZ ₁ |
|---------------|-----|-----|-----|-----|-----|-------|------------------|-------------------|
| B73 x Hp301 | 110 | 0.5 | 700 | 700 | 8.5 | 38.9 | 0.40 | 0.20 |
| B73_x_Mo17 | 110 | 0.5 | 700 | 700 | 5.9 | 38.9 | 0.20 | 0.15 |
| B73_x_NC338 | 110 | 0.5 | 700 | 700 | 7.8 | 38.9 | 0.65 | 0.40 |
| Mo17 x Hp301 | 110 | 0.5 | 700 | 700 | 5.5 | 38.9 | 0.10 | 0.10 |
| Mo17_x_NC338 | 110 | 0.5 | 700 | 700 | 8.5 | 38.9 | 0.50 | 0.30 |
| NC338_x_Hp301 | 110 | 0.5 | 700 | 700 | 5.1 | 38.9 | 0.10 | 0.10 |

Table 4: CROPGRO-Soybean cultivar and O₃ parameters used to simulate the seven soybean cultivars based on the maturity groups defined in the SoyFACE field experiment (Betzelberger et al., 2012). CSDL = Critical Short Day Length below which reproductive development progresses with no daylength effect (for shortday plants) (hour), PPSEN = Slope of the relative response of development to photoperiod with time (positive for shortday plants) (per hour), EM-FL = Time between plant emergence and flower appearance (R1) (photothermal days), FL-SH = Time between first flower and first pod (R3) (photothermal days), FL-SD = Time between first flower and first seed (R5) (photothermal days), SD-PM = Time between first seed (R5) and physiological maturity (R7) (photothermal days), FL-LF = Time between first flower (R1) and end of leaf expansion (photothermal days), LFMAX = Maximum leaf photosynthesis rate at 30 °C, 350 vpm CO₂, and high light (mg CO₂ m⁻² s⁻¹), SLAVR = Specific leaf area of cultivar under standard growth conditions (cm² g⁻¹), SIZLF = Maximum size of full leaf (three leaflets) (cm²), XFRT = Maximum fraction of daily growth that is partitioned to seed and shell, WTSPD = Maximum weight per seed (g), SFDUR = Seed filling duration for pod cohort at standard growth conditions (photothermal days), SDPDV = Average seed per pod under standard growing conditions (number per pod), PODUR = Time required for cultivar to reach final pod load under optimal conditions (photothermal days), THRSH = Threshing percentage. The maximum ratio of (seed per (seed + shell)) at maturity, SDPRO = Fraction protein in seeds (g(protein) per g(seed)), SLDLIP = Fraction oil in seeds (g(oil) per g(seed)), FOZ₁ = O₃ effect on photosynthesis, and SFOZ₁ = O₃ effect on leaf senescence.

| Cultivar | Maturity Group | CSDL | PPSEN | EM-FL | FL-SH | FL-SD | SD-PM | FL-LF | LFMAX | SLAVR | SIZLF | XFRT | WTSPD | SFDUR | SDPDV | PODUR | THRSH | SDPRO | SLDIP | FOZ ₁ | SFOZ ₁ |
|---------------|----------------|------|-------|-------|-------|-------|-------|-------|-------|-------|-------|------|-------|-------|-------|-------|-------|-------|-------|------------------|-------------------|
| Pioneer 93B15 | 3 | 13.1 | 0.285 | 19.0 | 6 | 14.0 | 33.2 | 26 | 1.20 | 375 | 180 | 1 | 0.16 | 23 | 2.2 | 10 | 77 | 0.405 | 0.205 | 0.25 | 0.25 |
| Dwight | 2 | 12.9 | 0.249 | 17.4 | 6 | 13.5 | 32.4 | 26 | 1.00 | 375 | 180 | 1 | 0.16 | 23 | 2.2 | 10 | 77 | 0.405 | 0.205 | 0.20 | 0.20 |
| HS93-4118 | 4 | 13.3 | 0.294 | 19.4 | 7 | 15.0 | 34.0 | 26 | 1.05 | 375 | 180 | 1 | 0.16 | 23 | 2.2 | 10 | 77 | 0.405 | 0.205 | 0.30 | 0.30 |
| IA-3010 | 3 | 13.2 | 0.285 | 19.0 | 6 | 14.0 | 33.2 | 26 | 1.01 | 375 | 180 | 1 | 0.16 | 23 | 2.2 | 10 | 77 | 0.405 | 0.205 | 0.25 | 0.25 |
| LN97-15076 | 4 | 13.2 | 0.294 | 19.4 | 7 | 15.0 | 34.0 | 26 | 1.08 | 375 | 180 | 1 | 0.19 | 23 | 2.2 | 10 | 77 | 0.405 | 0.205 | 0.30 | 0.30 |
| Loda | 2 | 12.7 | 0.249 | 17.4 | 6 | 13.5 | 32.4 | 26 | 1.03 | 375 | 180 | 1 | 0.19 | 23 | 2.2 | 10 | 77 | 0.405 | 0.205 | 0.30 | 0.30 |
| Pana | 3 | 13.0 | 0.285 | 19.0 | 6 | 14.0 | 33.2 | 26 | 1.00 | 375 | 180 | 1 | 0.15 | 23 | 2.2 | 10 | 77 | 0.405 | 0.205 | 0.25 | 0.30 |

Table 5: Observed and simulated anthesis day and maturity day for the six maize cultivars from the 2018 FACE experiment (Choquette et al., 2020) and the seven soybean cultivars from the 2009 and 2010 soybean SoyFACE experiments (Betzberger et al., 2012). The observed maturity dates were estimated from the single reported harvest date for all cultivars but there may have been minor variation between the different cultivars. Observed anthesis was not available for soybean.

| Crop experiment | Cultivar | Observed anthesis (dap) | Simulated anthesis (dap) | Observed maturity (dap) | Simulated maturity (dap) |
|-----------------|---------------|-------------------------|--------------------------|-------------------------|--------------------------|
| Maize 2018 | B73 x Hp301 | 48 | 48 | 97 | 97 |
| | B73 x Mo17 | 48 | 48 | 97 | 97 |
| | B73_x_NC338 | 48 | 48 | 97 | 97 |
| | Mo17 x Hp301 | 48 | 48 | 97 | 97 |
| | Mo17 x NC338 | 48 | 48 | 97 | 97 |
| | NC338 x Hp301 | 48 | 48 | 97 | 97 |
| Soybean 2009 | Pioneer93B15 | | 52 | 133 | 131 |
| | Dwight | | 48 | 133 | 126 |
| | HS93-4118 | | 53 | 133 | 133 |
| | IA-3010 | | 50 | 133 | 128 |
| | LN97-15076 | | 55 | 133 | 137 |
| | Loda | | 52 | 133 | 132 |
| | Pana | | 54 | 133 | 134 |
| Soybean 2010 | Pioneer93B15 | | 48 | 126 | 129 |
| | Dwight | | 44 | 126 | 125 |
| | HS93-4118 | | 48 | 126 | 129 |
| | IA-3010 | | 47 | 126 | 126 |
| | LN97-15076 | | 50 | 126 | 131 |
| | Loda | | 48 | 126 | 130 |
| | Pana | | 51 | 126 | 131 |

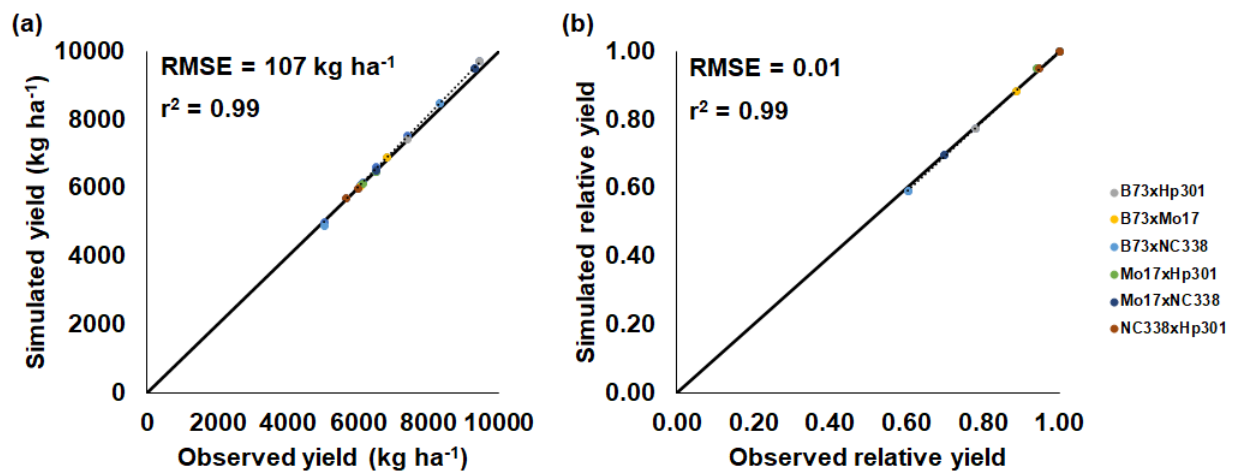
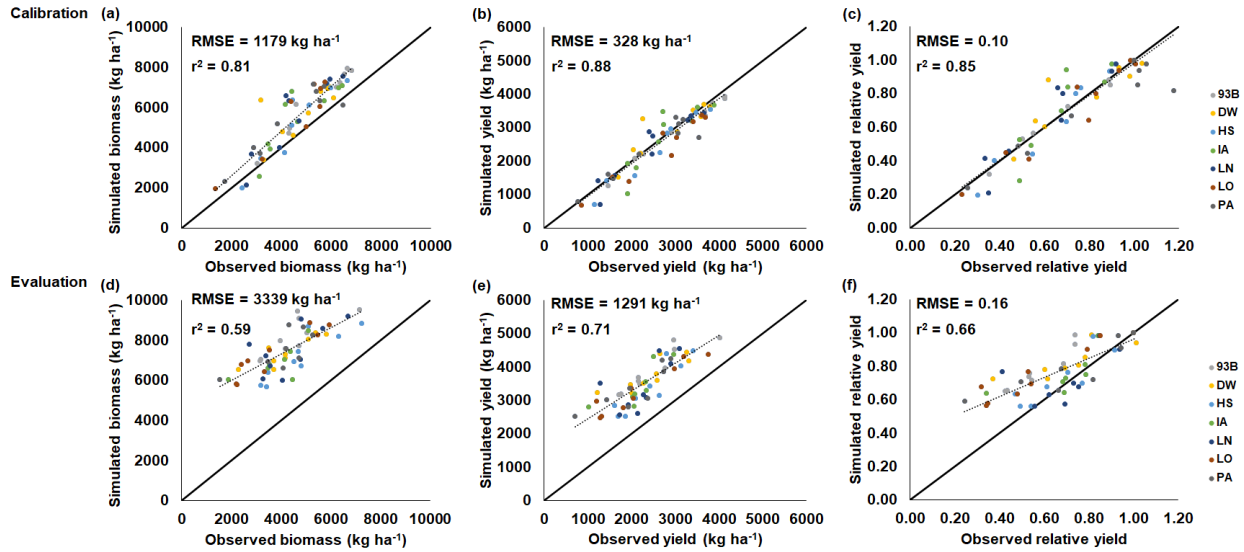


Figure 2: CERES-Maize model calibration of the 2018 FACE O₃ field experiment conducted in Champaign, Illinois, USA (Choquette et al., 2020). Simulated and observed (a) yield and (b) relative yield due to elevated O₃ stress (compared to the ambient control treatment) for six maize cultivars (colored points). The root-mean-square error (RMSE) and coefficient of determination (r^2) show the model performance across all cultivars. Solid black line shows 1:1 comparison and dotted black line shows linear fit across all cultivars. For maize only one year of experimental data was available for calibration and evaluation. The model cultivar parameters are shown in Table 3.



375

Figure 3: CROPGRO-Soybean model performance and evaluation of the SoyFACE O₃ field experiment conducted in Champaign, Illinois, USA (Betzberger et al., 2012). Simulated and observed (a, d) above-ground biomass, (b, e) yield, and (c, f) relative yield in response to the nine progressive O₃ increasing treatments (Table 2) for seven soybean cultivars (colored points). Relative yield is compared to the ambient control treatment within each year. The 2009 SoyFACE field experiment was used for model calibration (a, b, c), and the 2010 SoyFACE field experiment was used for model evaluation (d, e, f). The root-mean-square error (RMSE) and coefficient of determination (r^2) show the model performance across all cultivars. Solid black line shows 1:1 comparison and dotted black line shows linear fit across all cultivars. The model cultivar parameters are shown in Table 4.

380

3.2 Sensitivity analysis and combined effects of O₃, CO₂, and water deficit stress on yields

385

The simulated relative yield losses due to O₃ stress increased for all crops as the M7 O₃ concentrations increased above the 25 ppb threshold when examining the photosynthesis and leaf senescence responses independently, as expected (Figs. 4 – 7). The simulated actual yields for all crops are shown in the Supplementary Tables S2 – S9. Wheat was the most sensitive crop to O₃ stress of the four crops examined (compare slopes in Figs. 4 – 7 (a) and (b)) which agrees with previous literature (Mills et al., 2018a). For each model, simulations using a FOZ₁ or SFOZ₁ example value of 0.5 were examined in more detail to illustrate the O₃-CO₂-water interactions (Figs. 4 – 7 (c) and (d), respectively). For all crops, the Dry/reduced rainfall and low CO₂ treatment produced the lowest yields while the Wet/normal rainfall and high CO₂ produced the highest yields (Tables S2 – S9). The simulated O₃ effect was larger when water was non-limiting, i.e., the higher rainfall and irrigated treatments experienced larger losses due to O₃ stress because of increased stomatal uptake. The simulated O₃ effect was reduced under the higher CO₂ concentrations, thus capturing the responses from stomatal closure and the photosynthetic benefits from the CO₂ fertilization effect.

390

395

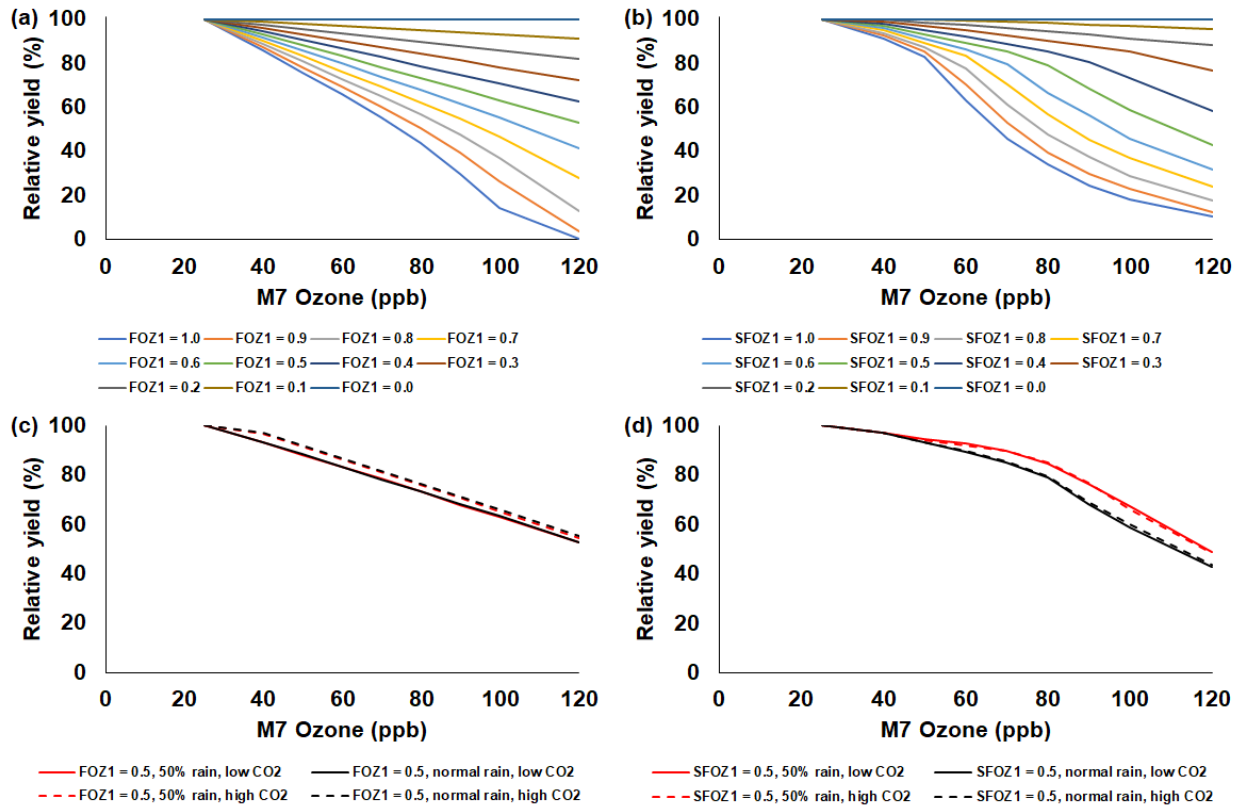
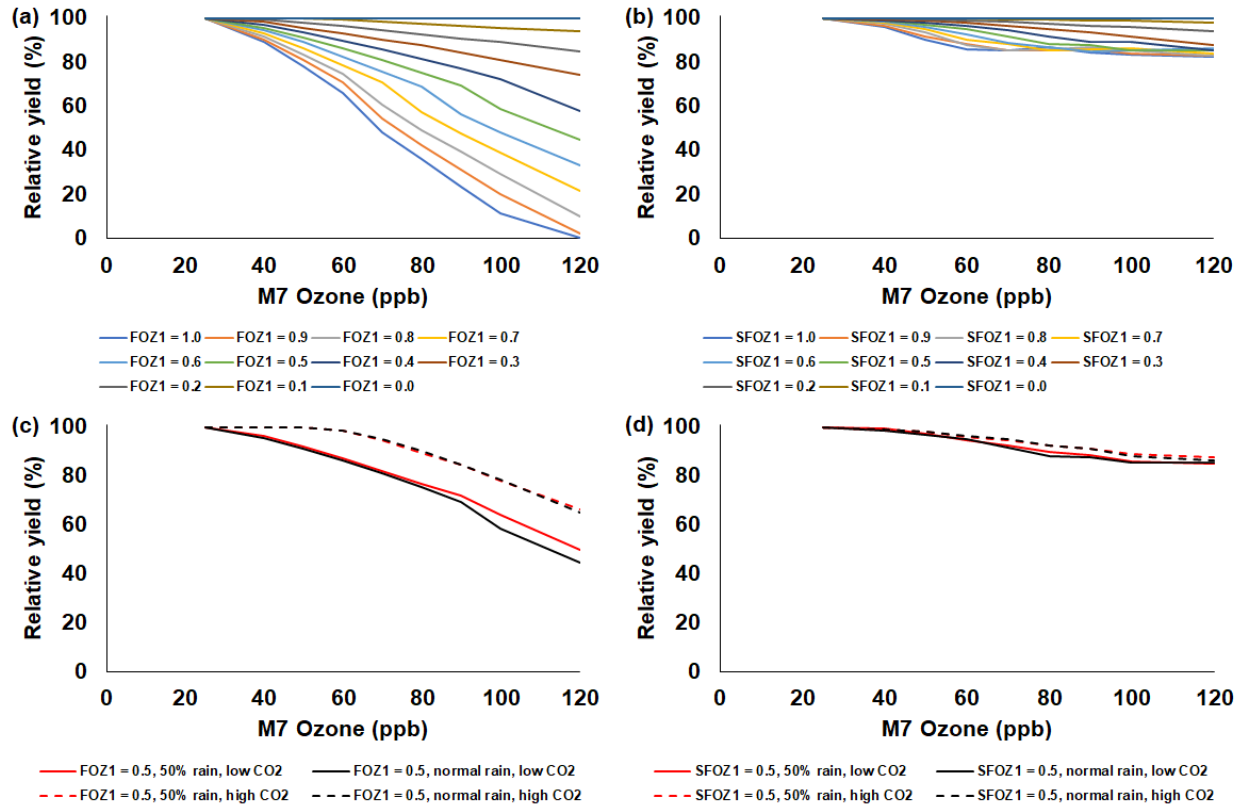


Figure 4: Sensitivity analysis using the CERES-Maize model to simulate relative yield due to elevated O₃ stress (relative to 25 ppb M7 O₃) for a range of (a) the photosynthesis O₃ stress parameter (FOZ₁) and (b) the leaf senescence O₃ stress parameter (SFOZ₁) values under the normal rainfall and 350 ppm CO₂ scenario, and an example of (c) FOZ₁ and (d) SFOZ₁ set at 0.5 under the 50% reduced rainfall and 350 ppm CO₂ (solid red line), normal rainfall and 350 ppm CO₂ (solid black line), 50% less rainfall and 550 ppm CO₂ (dashed red line), and normal rainfall and 550 CO₂ (dashed black line) scenarios. The Champaign, Illinois, USA 2018 FACE weather, soil, and dominant management conditions were used for the reference location. Each O₃ parameter was tested independently, i.e., when examining FOZ₁, SFOZ₁ was set to zero and vice versa. The simulated actual yields are shown in Tables S2 and S3.

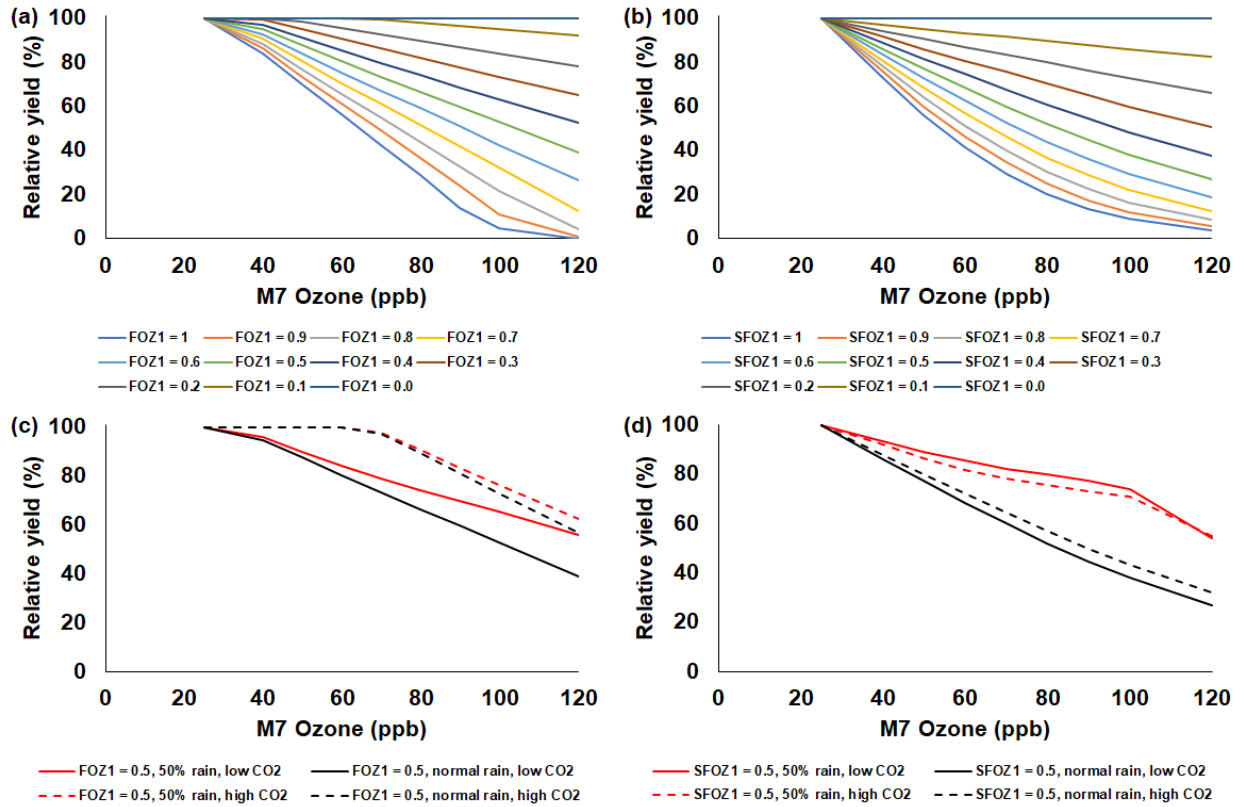
400



405

410

Figure 5: Sensitivity analysis using the CERES-Rice model to simulate relative yield due to elevated O_3 stress for a range of (a) FOZ_1 and (b) $SFOZ_1$ values under the normal rainfall and 350 ppm CO_2 scenario, and an example of (c) FOZ_1 and (d) $SFOZ_1$ set at 0.5 under the 50% reduced rainfall and 350 ppm CO_2 (solid red line), normal rainfall and 350 ppm CO_2 (solid black line), 50% less rainfall and 550 ppm CO_2 (dashed red line), and normal rainfall and 550 CO_2 (dashed black line) scenarios. The Stuttgart, Arkansas, USA 2009 weather, soil, and dominant management conditions were used for the reference location. Each O_3 parameter was tested independently, i.e., when examining FOZ_1 , $SFOZ_1$ was set to zero and vice versa. The simulated actual yields are shown in Tables S4 and S5.



415 **Figure 6: Sensitivity analysis using the CROPGRO-Soybean model to simulate relative yield due to elevated O₃ stress for**
a range of (a) FOZ₁ and (b) SFOZ₁ values under the normal rainfall and 350 ppm CO₂ scenario, and an example of (c)
FOZ₁ and (d) SFOZ₁ set at 0.5 under the 50% reduced rainfall and 350 ppm CO₂ (solid red line), normal rainfall and 350
ppm CO₂ (solid black line), 50% less rainfall and 550 ppm CO₂ (dashed red line), and normal rainfall and 550 CO₂
(dashed black line) scenarios. The Champaign, Illinois, USA 2009 SoyFACE weather, soil, and dominant management
conditions were used for the reference location. Each O₃ parameter was tested independently, i.e., when examining FOZ₁,
SFOZ₁ was set to zero and vice versa. The simulated actual yields are shown in Tables S6 and S7. Figure S6 shows the
relative biomass loss corresponding to SFOZ₁ (d) to explain the inverted CO₂ effect under the 50% rainfall treatment.
 420

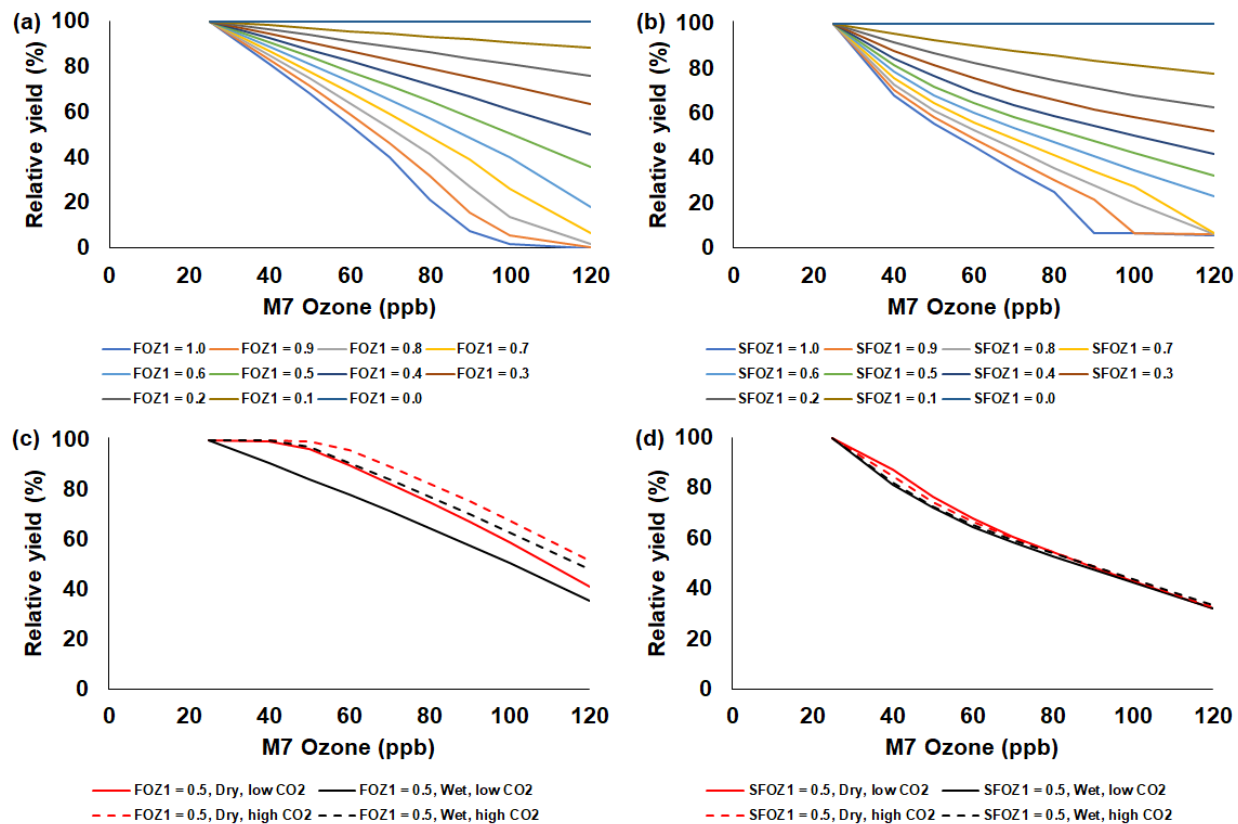


Figure 7: Sensitivity analysis using the NWheat model to simulate relative yield due to elevated O₃ stress for a range of (a) FOZ₁ and (b) SFOZ₁ values under the “Wet” irrigation and 350 ppm CO₂ scenario, and an example of (c) FOZ₁ and (d) SFOZ₁ set at 0.5 under the “Dry” irrigation and 350 ppm CO₂ (solid red line), “Wet” irrigation and 350 ppm CO₂ (solid black line), “Dry” irrigation and 550 ppm CO₂ (dashed red line), and “Wet” irrigation and 550 CO₂ (dashed black line) scenarios. The Maricopa, Arizona, USA 1993 FACE weather, soil, and management conditions were used for the reference location (Kimball et al., 1999; Guarin et al., 2019). Each O₃ parameter was tested independently, i.e., when examining FOZ₁, SFOZ₁ was set to zero and vice versa. The simulated actual yields are shown in Tables S8 and S9.

3.3 Simulated relative yield loss compared to O₃ relationships in the literature

For all crops, the literature showed a large range of relative yield losses due to O₃ stress caused by different cultivar O₃ sensitivities (Fig. S2). Wheat was the most sensitive crop to O₃ stress with an average yield loss of 0.70% ± 0.39 (mean ± SD) per ppb M7 O₃ increase above 25 ppb, followed by soybean, maize, and then rice (average yield losses of 0.60% ± 0.39, 0.39% ± 0.26, and 0.32% ± 0.37 per ppb M7 O₃ increase above 25 ppb, respectively) (average of slopes in Table S10). To encompass the high variability of yield losses, the cultivars were classified into the O₃ tolerant, intermediate, and sensitive cultivar O₃ sensitivities (Fig. S3). Since the cultivar sensitivities were not originally specified in the literature, the FOZ₁ and SFOZ₁ parameters used in the models were adjusted to provide the best fit across the O₃ exposure responses (Table 1). Overall, the models reproduced the simulated O₃ exposure relationships from the literature well; the RMSE for maize, rice, soybean, and wheat across all three O₃ exposure sensitivities were 6.6%, 7.8%, 4.0%, and 5.4%, respectively (Fig. 8). The models performed better (lower RMSE) for the O₃ tolerant and O₃ intermediate cultivar sensitivities compared to the O₃ sensitive cultivar sensitivity, but all

models explained the variance well ($r^2 > 0.96$ across all O_3 sensitivities). This suggests that different combinations of FOZ_1 and $SFOZ_1$ can be calibrated for specific observations to emulate the variation in different O_3 exposure responses.

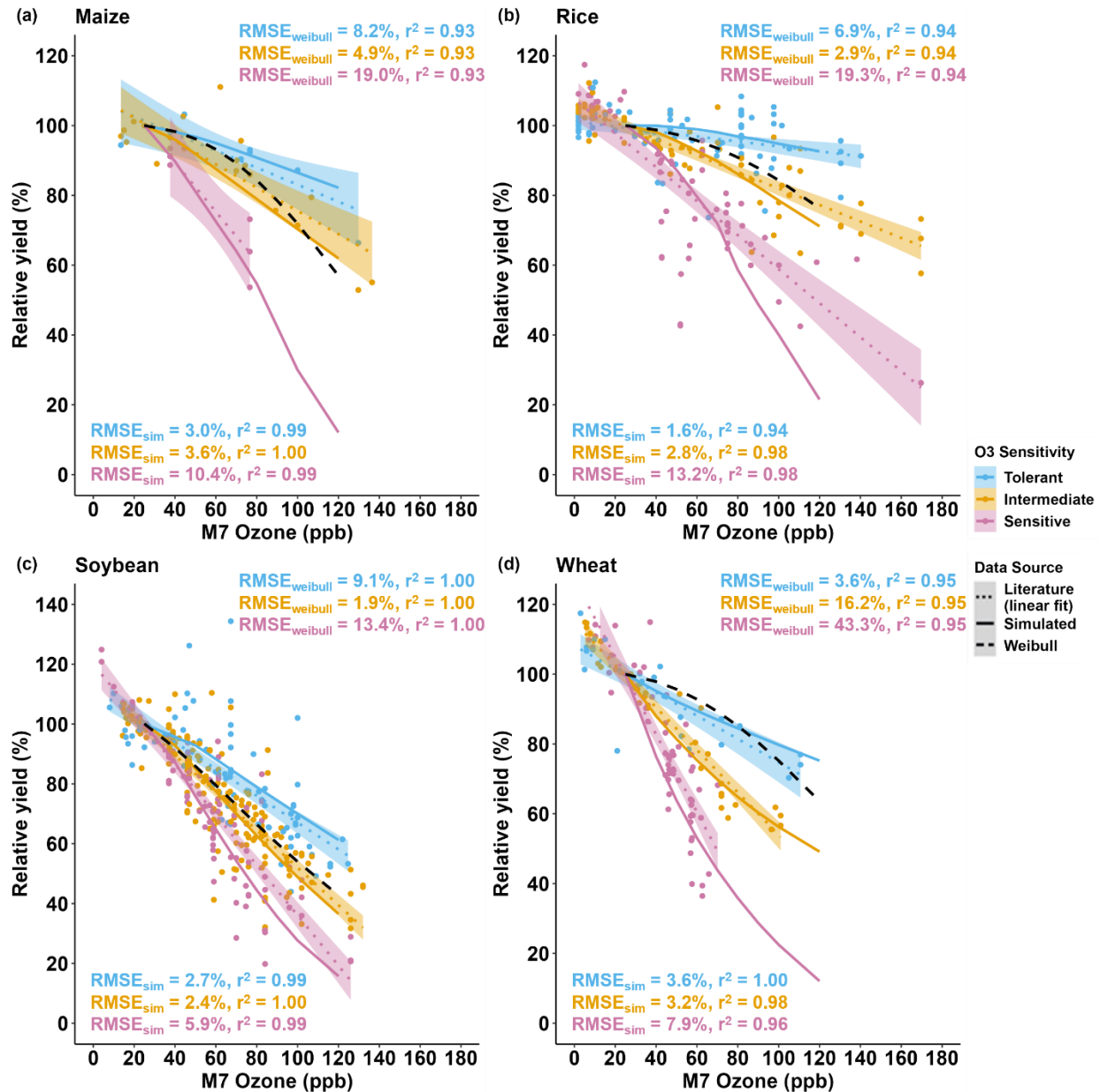


Figure 8: Simulated relative yield due to O_3 stress (solid lines) compared to the O_3 exposure relationships (dotted lines) from the literature data (symbols) for the (a) CERES-Maize, (b) CERES-Rice, (c) CROPGRO-Soybean, and (d) NWheat models. The calculated relative yield from the well-known Weibull O_3 response functions (dashed black lines, equations listed in Table S11) are based on the US NCLAN network O_3 exposure field experiments conducted between the 1960s to 1980s (Adams et al., 1989; Lesser et al., 1990; Wang and Mauzerall, 2004; Tai et al., 2021). The O_3 exposure-yield response linear fits of the three O_3 sensitivities: tolerant (blue), intermediate (gold), and sensitive (magenta) are given in Figure S3. The cultivars were classified by grouping the cultivar O_3 exposure-yield response (Fig. S2) into three evenly distributed quantiles: 66%-100%, 33%-66%, and 0%-33%, respectively. The O_3 sensitivities determined for each cultivar are listed in Table S10. The simulated results for the crop models use the FOZ_1 and $SFOZ_1$ values from Table 1. For each model, the same weather, soil, and dominant management conditions as in the normal rainfall and 350 ppm CO_2

460 treatment of the sensitivity analysis were used as reference (the O₃ response functions from the literature included O₃
field experiments conducted when the atmospheric CO₂ concentration was ~350 ppm). The literature data consists of the
relative yields (scaled to 25 ppb M7 O₃) of the cultivars examined in the Mills et al. (2018a) literature review combined
with the maize and soybean cultivars used in this study for a total of 9 maize cultivars, 50 rice cultivars, 49 soybean
cultivars, and 23 wheat cultivars (listed in Table S10). For the O₃ sensitivity of each crop, the root-mean-square error
465 (RMSE) and coefficient of determination (r^2) show the crop model performance (RMSE_{sim}) and the Weibull response
function performance (RMSE_{Weibull}) compared to the linear fit of the O₃ exposure literature data (text color corresponds
to O₃ sensitivity). The color shaded area shows the standard error for the linear fit of the literature data for each of the
cultivar O₃ sensitivities.

4 Discussion

4.1 Simulating O₃ damage on crop yields

470 The measured yield losses for the maize FACE experiment were between 5% to 40% for the M7 O₃ concentrations
when increasing from the ambient concentration (38 ppb) to the elevated O₃ treatment (77 ppb), a yield loss of 0.14%
to 1.01% per ppb M7 O₃ above the ambient concentration, depending on the O₃ cultivar sensitivity (Fig. 2b). Cv.
NC338xHp301 and cv. Mo17xHp301 were classified as O₃ tolerant because of relatively small yield losses of 5% and
6%, respectively; cv. B73xMo17 was classified as O₃ intermediate with a yield loss of 11%; and cv. B73xHp301, cv.
Mo17xNC338, and cv. B73xNC338 were sensitive to O₃ effects with yield losses of 22%, 30%, and 40%, respectively
475 (Fig. S1a, Table S10). These cultivar O₃ sensitivities are based on a single experimental year so additional testing is
needed to further corroborate the classifications. Overall, the calibrated CERES-Maize model was able to reproduce
these observed yield losses within 1%, i.e., simulated yield losses between 5% to 41%, or 0.12% to 1.05% per ppb O₃
increase above the ambient concentration. These yield losses were also calculated relative to 25 ppb (as described in
section 2.5) for consistency with the literature, which resulted in simulated yield losses between 0.12% to 0.93% per
480 ppb M7 O₃ increase above 25 ppb across the six cultivars.

When comparing the simulations to the maize O₃ exposure-yield relationships from the literature, the model simulated
average yield losses of 0.16%, 0.36%, and 0.82% per ppb M7 O₃ increase above 25 ppb for the O₃ tolerant,
intermediate, and sensitive cultivar O₃ sensitivities, respectively (Fig. 8 (a) solid lines). This agreed well with the
literature yield losses of 0.24%, 0.33%, and 0.71% per ppb M7 O₃ increase above 25 ppb for the O₃ tolerant,
485 intermediate, and sensitive cultivar sensitivities, respectively (Fig. S3 (a), Fig. 8 (a) dotted lines). The O₃ parameter
values used for the literature comparison were determined to provide the best fit across the literature experiments
consisting of nine maize cultivars, but these O₃ parameter values could be calibrated for other scenarios and cases,
i.e., higher or lower cultivar O₃ sensitivity.

490 The measured yield losses for the SoyFACE experiment were between 51% to 77% for the M7 O₃ concentrations
when increasing from the ambient concentration (37 ppb) to the highest O₃ treatment (126 ppb) in 2009, a yield loss
of 0.57% to 0.86% per ppb M7 O₃ above the ambient concentration, depending on the cultivar O₃ sensitivity (Fig. 3
(c)). The calibrated CROPGRO-Soybean model reproduced observed yields losses within 10%, i.e., simulated yield
losses between 59% to 80%, or 0.66% to 0.90% per ppb O₃ increase. Based on the calculated O₃ classifications from
the literature and low yield divergence across the seven cultivars (Fig. S1 (b)), cv. Pioneer93B15, cv. Dwight, cv. IA-
495 3010, and LN97-15076 were considered O₃ intermediate sensitivity, and cv. HS93-4118, cv. Loda, and cv. Pana were
considered O₃ sensitive (Table S10). In 2010, the observed soybean yield losses ranged between 31% to 76% when

increasing from the ambient concentration (37 ppb) to the highest O₃ treatment (84 ppb), a yield loss of 0.65% to 1.60% per ppb M7 O₃ above the ambient concentration. The model underestimated yield losses in 2010, between 27% to 44%, but because the experimental setup was the same for both years, an external factor may have affected yields that was not considered in the simulations (section 4.3). The 2010 yield losses were a similar magnitude to the 2009 yield losses, but the 2010 experiment had higher yield loss and variation per ppb O₃ increase with lower average M7 O₃ concentrations (Table 2, Fig. S4 (a)).

When comparing the simulations to the soybean O₃ exposure-yield relationships from the literature (Fig. 8 (c)), an average yield loss of 0.36%, 0.64%, and 0.96% per ppb M7 O₃ increase above 25 ppb was simulated for the O₃ tolerant, intermediate, and sensitive cultivar O₃ sensitivities, respectively. This was substantiated by the literature yield losses of 0.45%, 0.63%, and 0.84% per ppb M7 O₃ increase above 25 ppb for the O₃ tolerant, intermediate, and sensitive cultivar O₃ sensitivities, respectively (Fig. S3 (c), Fig. 8 (c) dotted lines). The literature data consisted of 49 soybean cultivars, which had a smaller range of O₃ sensitivities compared to the other crops, although there were outliers where yield increased under higher O₃ concentrations (described in section 4.2).

The CERES-Rice model simulated an average yield loss of 0.05%, 0.23%, and 0.66% per ppb M7 O₃ increase above 25 ppb for the O₃ tolerant, intermediate, and sensitive cultivar O₃ sensitivities, respectively (Fig. 8 (b) solid lines). The rice literature had the most cultivars (50) of the four crops examined, and the simulated yield losses for the O₃ tolerant and intermediate cultivar O₃ sensitivities agreed well with the literature yield losses of 0.07% and 0.24% per ppb M7 O₃ increase above 25 ppb, respectively (Fig. 8 (b) dotted lines). A larger discrepancy between the simulated yield loss for the O₃ sensitive classification and the literature O₃ sensitive yield loss of 0.49% per ppb M7 O₃ increase above 25 ppb was due to the higher variability within the literature data (Fig. 8 (b) shaded area).

Using the calibrated NWheat model, the simulated yield losses were 0.26%, 0.66%, and 1.23% per ppb M7 O₃ increase above 25 ppb for the O₃ tolerant, intermediate, and sensitive cultivar O₃ sensitivities, respectively (Fig 8 (d)). These simulated yield losses were corroborated by the reported average yield losses of 0.33%, 0.61%, and 1.11% per ppb M7 O₃ increase above 25 ppb for the O₃ tolerant, intermediate, and sensitive cultivar O₃ sensitivities, respectively. The literature expanded across different ranges of O₃ concentrations for all crops, and yield loss per ppb is not always constant over an expansive range of O₃ concentrations, so the model O₃ parameter values can be adjusted for higher or lower cultivar O₃ sensitivity.

As an additional check of model performance, the calculated relative yield from the well-known Weibull O₃ response functions (Table S11) were compared to the literature O₃ exposure linear yield responses for each crop and O₃ classification (Fig. 8). The Weibull function performance was then compared to the simulated crop model results. Overall, the crop model simulations performed better (lower RMSE and higher r²) than the Weibull response functions across all crops for all three O₃ classifications, except the O₃ intermediate classification for soybean which had < 1% difference between the RMSE (compare RMSE and r² in Fig. 8). The performance results suggest that it is best to use calibrated crop models when available, and that the Weibull response functions are mainly representative of O₃ intermediate classifications for maize, rice, and soybean, and O₃ tolerant classifications for wheat.

4.2 Simulated relative yield loss with the combined effects of O₃, CO₂, and water deficit stress

The sensitivity analyses showed that the yield losses due to O₃ stress were higher under the normal rainfall and low CO₂ treatment which agrees with previous literature that increased water availability increases O₃ impact due to increased stomatal uptake (Khan and Soja, 2003; Biswas et al., 2013). It was unexpected that the simulated O₃ photosynthetic response difference between the normal and reduced rainfall treatments for maize was less than 1% (Fig. 4 (c)). This was because the model simulated low water deficit stress under the 50% reduced rainfall treatment which obscured the O₃-water stress dynamics. Further reducing the rainfall to 40% of the normal amount increased the simulated water deficit stress and produced the photosynthetic O₃-water dynamics consistent with the other models (Fig. S5). The elevated CO₂ concentration mitigated the detrimental effect of O₃ stress in the photosynthetic response for all models (Figs. 4 – 7 (c)), which agrees with recent global findings that elevated CO₂ concentrations can mitigate and even negate elevated O₃ impacts (Xia et al., 2021; Tai et al., 2021). Interestingly, the CROPGRO-Soybean model simulated an inverse O₃-CO₂ effect on relative yield under the 50% rainfall condition when examining SFOZ₁ in detail (Fig. 6 (d)). This inverse yield response was due to the low actual yield simulated under the 50% rainfall and low CO₂ treatment (< 2,000 kg ha⁻¹, Table S7) which resulted in smaller changes in yield compared to the 50% rainfall and high CO₂ treatment, but the overall simulated aboveground biomass O₃-CO₂-water interaction was as expected (Fig. S6).

For several of the observations from the actual soybean field experiment using cv. Pana, the yield increased under higher O₃ concentrations (~2% to 18%, Fig. 3 (c) and Fig. S1 (b)). In some cases it is possible that elevated O₃ concentrations can benefit a crop via hormesis, a process where low levels of intermittent stress may benefit overall crop growth through improved resiliency (Calabrese, 2014). It is also possible that if elevated O₃ concentrations reduce biomass growth throughout the season, and therefore reduce nutrient resource demand throughout the season, small yield increases can occur from a larger pool of resources available during the key reproductive/grain filling period (Asseng and Van Herwaarden, 2003; Guarin et al., 2019). This increase in yield under higher O₃ concentrations was also observed under several other soybean and rice cultivars from the literature (Fig. S2 (b) and (c)). However, a soybean cultivar from the literature, cv. Cumberland, was reported to have a 34% increase under elevated O₃ (67 ppb) compared to the control treatment (25 ppb), but such a large increase may indicate that another outside factor affected the yields. The experimentalists speculated that the large yield difference was due to changes in the seasonal water dynamics thereby causing increased drought stress under the control treatment compared to the elevated O₃ treatment (Mulchi et al., 1988).

4.3 Uncertainty in model simulations and O₃ exposure field experiments

Crop models contain uncertainties due to simplification of complex biological processes, but field experiments may also contribute uncertainty via measurement. The soybean simulations overestimated both biomass and yield across all cultivars and treatments for the 2010 SoyFACE experiment. Since both the ambient and elevated O₃ treatments were overestimated, it is unlikely that the simulated O₃ interactions caused the discrepancy. Examining the weather input showed a 14% increase in cumulative incoming solar radiation for the 2010 growing season compared to the 2009 growing season (Fig. S4 (b)). The 2010 season was warmer than the 2009 season, average seasonal temperature of 23.4 °C compared to 19.1 °C, but no heat stress was reported and the difference in rainfall was negligible, 445 mm

570 compared to 454 mm. Since management was the same for both years and no water or N stresses were reported, it was
575 expected that the 2010 yields would be higher than the 2009 yields due to the increased solar radiation, but the average
2010 yield across all cultivars for the ambient treatment decreased, 3300 kg ha⁻¹ in 2010 compared to 3700 kg ha⁻¹ in
2009. Therefore, it is possible that an outside stress factor not considered within the model limited soybean growth in
the field in 2010 which led to the model overestimating biomass and yield. One possibility is that increased rainfall
during the beginning of the 2010 season (221 mm in first 30 days compared to 153 mm in first 30 days of 2009 season,
Fig. S4 (c)) may have resulted in germination or emergence stress due to excessive water such as flooding or lodging,
which are factors not yet considered in the crop models.

The sensitivity analyses showed that the CO₂ effect was more pronounced in the model photosynthesis response than
in the leaf senescence response (compare solid and dashed lines in Figs. 4 – 7 (c) and (d)). This is because the models
do not have a CO₂ effect directly applied to the daily leaf senescence calculation, whereas CO₂ directly affects the
580 daily photosynthesis calculation (PCARB in Eq. (3) and (4), and PRATIO in Eq. (9)). Improved CO₂ representation
within the crop models is being explored through the Agricultural Model Intercomparison and Improvement Project
(AgMIP) studies (Ahmed et al., 2017; Ahmed et al., 2019; Toreti et al., 2020), but additional high-quality data is
needed for model testing.

5 Conclusion

585 Crop responses to elevated O₃ concentrations were incorporated into the DSSAT CERES-Maize, CERES-Rice,
CROPGRO-Soybean, and NWheat crop models via functions reducing photosynthetic activity and accelerating leaf
senescence. Model testing showed that each of the four models reproduced the observed O₃ response from field
experiments and previous literature, as well as the expected interactions between O₃, CO₂, and water deficit stress.
The simulated yield responses were also more representative of the O₃ exposure literature data than the well-known
590 Weibull O₃ response functions for all crops. Thus, this incorporation allows for improved simulation of the
heterogeneity of O₃ impacts across geographical regions and systems, as well as across years within seasons, which is
more representative of real-world interactions than using a generic damage coefficient. Overall, increasing M7 O₃
concentrations had a negative effect on growth and yield across all four crops, and this negative effect was exacerbated
by increased water availability and ameliorated by elevated CO₂ concentrations. The O₃ impact and stress response of
595 the crop depends on the stress severity, duration, frequency, cultivar sensitivity, and seasonal timing (i.e.,
developmental stage) which can be accounted for by using the updated crop models.

The addition of O₃ stress functionality into crop models will improve both near- and long-term simulations of global
environmental interactions using a key factor that is often not included in agricultural and climate change assessments.
The DSSAT models in this study can be used to simulate the O₃ impacts on crops in combination with climate change.
600 The O₃ parameter values in this study can be used as preliminary approximations, but to further improve model
performance and robustness of the O₃ stress routines, the models and parameters should continue to be tested and
calibrated with additional O₃ exposure experimental data when available. In addition, the models should be compared
with other O₃-modified crop models as part of multi-model ensemble intercomparison and improvement assessments
conducted by the AgMIP (<https://agmip.org/>). As a next step, the AgMIP Ozone team is currently conducting a multi-

605 model ensemble study with crop models that have the capacity to evaluate the responses of future crop yields to
different ozone concentrations. This effort will help produce more robust estimates of climate change impacts in global
agriculture. The framework described here can be used by other process-based crop models, local or gridded, to
incorporate O₃ stress interactions into the model. This model improvement also suggests potential future collaboration
610 between crop modelers and remote sensing experts using weather and climate models with dynamic chemistry
components, such as the NASA Atmosphere Observing System (<https://aos.gsfc.nasa.gov/>).

Code availability

The current version of the DSSAT crop modeling platform is available to download from the DSSAT Foundation
website (<https://dssat.net/>). The current version of the pSIMS framework is available to download from the RDCEP
website (<http://www.rdcep.org/research-projects/psims>). The O₃-modified version of the DSSAT crop models will be
615 available with the next DSSAT version release, and the O₃-modified version of the pDSSAT crop models is available
from the GitHub repository at https://github.com/jguarin4/dssat-csm-os/tree/develop_v4.8_pdssat. An archived
version of the code is also available on Zenodo at <https://zenodo.org/badge/latestdoi/232137043>. The R code used to
classify the cultivar O₃ sensitivities is available on the Harvard Dataverse at <https://doi.org/10.7910/DVN/0NN9MH>.

Data availability

620 All field experimental and literature data used in this study are available from the sources referenced. The crop model
simulated output data is available on the Harvard Dataverse at <https://doi.org/10.7910/DVN/0NN9MH>.

Author Contribution

J.R.G. and J.J. designed and conducted the study. E.A.A. provided the O₃ exposure field data. K.S. collated the O₃
exposure literature data. J.R.G. and F.O. incorporated the O₃ modifications into the DSSAT/pDSSAT model code.
625 S.A., K.B., L.E., G.H., and A.C.R. provided insight on O₃-crop interactions within the crop models. J.E., I.F., and
D.K. provided technical support and guidance for the pSIMS/pDSSAT framework. J.R.G. and J.J. co-wrote the
manuscript. All authors contributed to editing the manuscript.

Competing interests

The authors declare that they have no conflict of interest.

630 Acknowledgements

The authors would like to thank Amy Betzelberger and Nicole Choquette for sharing the O₃ field experiment data.
J.R.G. and K.S. would like to thank Stephanie Osborne for help with collecting the O₃ exposure literature data. J.R.G.

and J.J. were supported by the Open Philanthropy Project. J.R.G., J.J. and A.C.R. contributions were also enabled by NASA Earth Science Division support of the NASA GISS Climate Impacts Group.

635 **References**

- Adams, R. M., Glycer, J. D., Johnson, S. L., and McCarl, B. A.: A reassessment of the economic effects of ozone on United States agriculture, *Japca-the Journal of the Air & Waste Management Association*, 39, 960-968, 10.1080/08940630.1989.10466583, 1989.
- 640 Ahmed, M., Stockle, C. O., Nelson, R., and Higgins, S.: Assessment of Climate Change and Atmospheric CO₂ Impact on Winter Wheat in the Pacific Northwest Using a Multimodel Ensemble, *Frontiers in Ecology and Evolution*, 5, 10.3389/fevo.2017.00051, 2017.
- Ahmed, M., Stockle, C. O., Nelson, R., Higgins, S., Ahmad, S., and Raza, M. A.: Novel multimodel ensemble approach to evaluate the sole effect of elevated CO₂ on winter wheat productivity, *Scientific Reports*, 9, 10.1038/s41598-019-44251-x, 2019.
- 645 Ainsworth, E. A.: Understanding and improving global crop response to ozone pollution, *Plant Journal*, 90, 886-897, 10.1111/tbj.13298, 2017.
- Arias, P. A., Bellouin, N., Coppola, E., Jones, R. G., Krinner, G., Marotzke, J., Naik, V., Palmer, M. D., Plattner, G.-K., Rogelj, J., Rojas, M., Sillmann, J., Storelvmo, T., Thorne, P. W., Trewin, B., Achuta Rao, K., Adhikary, B., Allan, R. P., Armour, K., Bala, G., Barimalala, R., Berger, S., Canadell, J. G., Cassou, C., Cherchi, A., Collins, W., 650 Collins, W. D., Connors, S. L., Corti, S., Cruz, F., Dentener, F. J., Dereczynski, C., Di Luca, A., Diongue Niang, A., Doblas-Reyes, F. J., Dosio, A., Douville, H., Engelbrecht, F., Eyring, V., Fischer, E., Forster, P., Fox-Kemper, B., Fuglestedt, J. S., Fyfe, J. C., Gillett, N. P., Goldfarb, L., Gorodetskaya, I., Gutierrez, J. M., Hamdi, R., Hawkins, E., Hewitt, H. T., Hope, P., Islam, A. S., Jones, C., Kaufman, D. S., Kopp, R. E., Kosaka, Y., Kossin, J., Krakovska, S., Lee, J.-Y., Li, J., Mauritsen, T., Maycock, T. K., Meinshausen, M., Min, S.-K., Monteiro, P. M. S., Ngo-Duc, T., 655 Otto, F., Pinto, I., Pirani, A., Raghavan, K., Ranasinghe, R., Ruane, A. C., Ruiz, L., Sallée, J.-B., Samset, B. H., Sathyendranath, S., Seneviratne, S. I., Sörensson, A. A., Szopa, S., Takayabu, I., Tréguier, A.-M., van den Hurk, B., Vautard, R., von Schuckmann, K., Zaehle, S., Zhang, X., and Zickfeld, K.: 2021: Technical Summary, in: *Climate Change 2021: The Physical Science Basis. Contribution of Working Group I to the Sixth Assessment Report of the Intergovernmental Panel on Climate Change*, edited by: Masson-Delmotte, V., Zhai, P., Pirani, A., Connors, S. L., Péan, C., Berger, S., Caud, N., Chen, Y., Goldfarb, L., Gomis, M. I., Huang, M., Leitzell, K., Lonnoy, E., Matthews, J. B. R., Maycock, T. K., Waterfield, T., Yelekçi, O., Yu, R., and Zhou, B., Cambridge University Press, Cambridge, United Kingdom and New York, NY, USA, 33-144, 10.1017/9781009157896.002, 2021.
- Asseng, S. and van Herwaarden, A. F.: Analysis of the benefits to wheat yield from assimilates stored prior to grain filling in a range of environments, *Plant and Soil*, 256, 217-229, 10.1023/a:1026231904221, 2003.
- 665 Asseng, S., Jamieson, P. D., Kimball, B., Pinter, P., Sayre, K., Bowden, J. W., and Howden, S. M.: Simulated wheat growth affected by rising temperature, increased water deficit and elevated atmospheric CO₂, *Field Crops Research*, 85, 85-102, 10.1016/s0378-4290(03)00154-0, 2004.
- Asseng, S., Ewert, F., Martre, P., Rotter, R. P., Lobell, D. B., Cammarano, D., Kimball, B. A., Ottman, M. J., Wall, G. W., White, J. W., Reynolds, M. P., Alderman, P. D., Prasad, P. V. V., Aggarwal, P. K., Anothai, J., Basso, B., 670 Biernath, C., Challinor, A. J., De Sanctis, G., Doltra, J., Fereres, E., Garcia-Vile, M., Gayler, S., Hoogenboom, G., Hunt, L. A., Izaurrealde, R. C., Jabloun, M., Jones, C. D., Kersebaum, K. C., Koehler, A. K., Muller, C., Kumar, S. N., Nendel, C., O'Leary, G., Olesen, J. E., Palosuo, T., Priesack, E., Rezaei, E. E., Ruane, A. C., Semenov, M. A., Shcherbak, I., Stockle, C., Stratonovitch, P., Streck, T., Supit, I., Tao, F., Thorburn, P. J., Waha, K., Wang, E., Wallach, D., Wolf, I., Zhao, Z., and Zhu, Y.: Rising temperatures reduce global wheat production, *Nature Climate Change*, 5, 143-147, 10.1038/nclimate2470, 2015.
- 675 Bassu, S., Brisson, N., Durand, J. L., Boote, K., Lizaso, J., Jones, J. W., Rosenzweig, C., Ruane, A. C., Adam, M., Baron, C., Basso, B., Biernath, C., Boogaard, H., Conijn, S., Corbeels, M., Deryng, D., De Sanctis, G., Gayler, S., Grassini, P., Hatfield, J., Hoek, S., Izaurrealde, C., Jongschaap, R., Kemanian, A. R., Kersebaum, K. C., Kim, S. H., Kumar, N. S., Makowski, D., Muller, C., Nendel, C., Priesack, E., Pravia, M. V., Sau, F., Shcherbak, I., Tao, F., 680 Teixeira, E., Timlin, D., and Waha, K.: How do various maize crop models vary in their responses to climate change factors?, *Global Change Biology*, 20, 2301-2320, 10.1111/gcb.12520, 2014.
- Betzberger, A. M., Yendrek, C. R., Sun, J. D., Leisner, C. P., Nelson, R. L., Ort, D. R., and Ainsworth, E. A.: Ozone Exposure Response for U.S. Soybean Cultivars: Linear Reductions in Photosynthetic Potential, Biomass, and Yield, *Plant Physiology*, 160, 1827-1839, 10.1104/pp.112.205591, 2012.

- 685 Biswas, D. K., Xu, H., Li, Y. G., Ma, B. L., and Jiang, G. M.: Modification of photosynthesis and growth responses to elevated CO₂ by ozone in two cultivars of winter wheat with different years of release, *Journal of Experimental Botany*, 64, 1485-1496, 10.1093/jxb/ert005, 2013.
- Boote, K. J. and Pickering, N. B.: Modeling photosynthesis of row crop canopies, *Hortscience*, 29, 1423-1434, 10.21273/hortsci.29.12.1423, 1994.
- 690 Calabrese, E. J.: Hormesis: a fundamental concept in biology, *Microbial Cell*, 1, 145-149, 10.15698/mic2014.05.145, 2014.
- Choquette, N. E., Ainsworth, E. A., Bezodis, W., and Cavanagh, A. P.: Ozone tolerant maize hybrids maintain Rubisco content and activity during long-term exposure in the field, *Plant Cell and Environment*, 43, 3033-3047, 10.1111/pce.13876, 2020.
- 695 Cooper, O. R., Parrish, D. D., Ziemke, J., Balashov, N. V., Cupeiro, M., Galbally, I. E., Gilge, S., Horowitz, L., Jensen, N. R., Lamarque, J.-F., Naik, V., Oltmans, S. J., Schwab, J., Shindell, D. T., Thompson, A. M., Thouret, V., Wang, Y., and Zbinden, R. M.: Global distribution and trends of tropospheric ozone: An observation-based review, *Elementa Science of the Anthropocene*, 2, <http://doi.org/10.12952/journal.elementa.000029>, 2014.
- Elliott, J., Kelly, D., Chryssanthacopoulos, J., Glotter, M., Jhunjhnuwala, K., Best, N., Wilde, M., and Foster, I.: The parallel system for integrating impact models and sectors (pSIMS), *Environmental Modelling & Software*, 62, 509-516, 10.1016/j.envsoft.2014.04.008, 2014.
- 700 Emberson, L.: Effects of ozone on agriculture, forests and grasslands, *Philosophical Transactions of the Royal Society a-Mathematical Physical and Engineering Sciences*, 378, 27, 10.1098/rsta.2019.0327, 2020.
- Emberson, L. D., Pleijel, H., Ainsworth, E. A., van den Berg, M., Ren, W., Osborne, S., Mills, G., Pandey, D., 705 Dentener, F., Buker, P., Ewert, F., Koeble, R., and Van Dingenen, R.: Ozone effects on crops and consideration in crop models, *European Journal of Agronomy*, 100, 19-34, 10.1016/j.eja.2018.06.002, 2018.
- Feng, Z. Z. and Kobayashi, K.: Assessing the impacts of current and future concentrations of surface ozone on crop yield with meta-analysis, *Atmospheric Environment*, 43, 1510-1519, 10.1016/j.atmosenv.2008.11.033, 2009.
- Feng, Z. Z., Xu, Y. S., Kobayashi, K., Dai, L. L., Zhang, T. Y., Agathokleous, E., Calatayud, V., Paoletti, E., 710 Mukherjee, A., Agrawal, M., Park, R. J., Oak, Y. J., and Yue, X.: Ozone pollution threatens the production of major staple crops in East Asia, *Nature Food*, 3, 47-+, 10.1038/s43016-021-00422-6, 2022.
- Griffiths, P. T., Murray, L. T., Zeng, G., Shin, Y. M., Abraham, N. L., Archibald, A. T., Deushi, M., Emmons, L. K., Galbally, I. E., Hassler, B., Horowitz, L. W., Keeble, J., Liu, J., Moeini, O., Naik, V., O'Connor, F. M., Oshima, N., Tarasick, D., Tilmes, S., Turnock, S. T., Wild, O., Young, P. J., and Zanis, P.: Tropospheric ozone in CMIP6 715 simulations, *Atmospheric Chemistry and Physics*, 21, 4187-4218, 10.5194/acp-21-4187-2021, 2021.
- Guarin, J. R., Kassie, B., Mashhaet, A. M., Burkey, K., and Asseng, S.: Modeling the effects of tropospheric ozone on wheat growth and yield, *European Journal of Agronomy*, 105, 13-23, 10.1016/j.eja.2019.02.004, 2019.
- Heck, W. W., Cure, W. W., Rawlings, J. O., Zaragoza, L. J., Heagle, A. S., Heggstad, H. E., Kohut, R. J., Kress, L. W., and Temple, P. J.: Assessing impacts of ozone on agricultural crops: 2. Crop yield functions and alternative 720 exposure statistics, *Journal of the Air Pollution Control Association*, 34, 810-817, 10.1080/00022470.1984.10465815, 1984.
- Hoogenboom, G., Porter, C. H., Boote, K. J., Shelia, V., Wilkens, P. W., Singh, U., White, J. W., Asseng, S., Lizaso, J. I., Moreno, L. P., Pavan, W., Ogoshi, R., Hunt, L. A., Tsuji, G. Y., and Jones, J. W.: The DSSAT crop modeling ecosystem, in: *Advances in Crop Modeling for a Sustainable Agriculture*, edited by: Boote, K. J., Burleigh 725 Dodds Science Publishing, Cambridge, United Kingdom, 173-216, 10.19103/AS.2019.0061.10, 2019.
- Hou, P. and Wu, S. L.: Long-term Changes in Extreme Air Pollution Meteorology and the Implications for Air Quality, *Scientific Reports*, 6, 9, 10.1038/srep23792, 2016.
- Hunsaker, D. J., Kimball, B. A., Pinter, P. J., LaMorte, R. L., and Wall, G. W.: Carbon dioxide enrichment and irrigation effects on wheat evapotranspiration and water use efficiency, *Transactions of the Asae*, 39, 1345-1355, 730 1996.
- IPCC: *Climate Change 2021: The Physical Science Basis. Contribution of Working Group I to the Sixth Assessment Report of the Intergovernmental Panel on Climate Change*, 2021.
- Jagermeyr, J., Muller, C., Ruane, A. C., Elliott, J., Balkovic, J., Castillo, O., Faye, B., Foster, I., Folberth, C., Franke, J. A., Fuchs, K., Guarin, J. R., Heinke, J., Hoogenboom, G., Iizumi, T., Jain, A. K., Kelly, D., Khabarov, N., 735 Lange, S., Lin, T. S., Liu, W. F., Mialyk, O., Minoli, S., Moyer, E. J., Okada, M., Phillips, M., Porter, C., Rabin, S. S., Scheer, C., Schneider, J. M., Schyns, J. F., Skalsky, R., Smerald, A., Stella, T., Stephens, H., Webber, H., Zabel, F., and Rosenzweig, C.: Climate impacts on global agriculture emerge earlier in new generation of climate and crop models, *Nature Food*, 2, 875-+, 10.1038/s43016-021-00400-y, 2021.
- Jones, C. A. and Kiniry, J. R.: *CERES-Maize: A simulation model of maize growth and development*, Texas A&M 740 University Press, College Station, TX1986.

- Jones, J. W., Hoogenboom, G., Porter, C. H., Boote, K. J., Batchelor, W. D., Hunt, L. A., Wilkens, P. W., Singh, U., Gijssman, A. J., and Ritchie, J. T.: The DSSAT cropping system model, *European Journal of Agronomy*, 18, 235-265, 10.1016/s1161-0301(02)00107-7, 2003.
- 745 Khan, S. and Soja, G.: Yield responses of wheat to ozone exposure as modified by drought-induced differences in ozone uptake, *Water Air and Soil Pollution*, 147, 299-315, 10.1023/a:1024577429129, 2003.
- Kimball, B. A., LaMorte, R. L., Pinter, P. J., Wall, G. W., Hunsaker, D. J., Adamsen, F. J., Leavitt, S. W., Thompson, T. L., Matthias, A. D., and Brooks, T. J.: Free-air CO₂ enrichment and soil nitrogen effects on energy balance and evapotranspiration of wheat, *Water Resources Research*, 35, 1179-1190, 10.1029/1998wr900115, 1999.
- 750 Kimball, B. A., Pinter Jr., P. J., LaMorte, R. L., Leavitt, S. W., Hunsaker, D. J., Wall, G. W., Wechsung, F., Wechsung, G., Bloom, A. J., and White, J. W.: Data from the Arizona FACE (free-air CO₂ enrichment) experiments on wheat at ample and limiting levels of water and nitrogen, *Open Data Journal for Agricultural Research*, 3, 29-38, <https://doi.org/10.18174/odjar.v3i1.15826>, 2017.
- 755 Kothari, K., Battisti, R., Boote, K. J., Archontoulis, S. V., Confalone, A., Constantin, J., Cuadra, S. V., Debaeke, P., Faye, B., Grant, B., Hoogenboom, G., Jing, Q., van der Laan, M., da Silva, F. A. M., Marin, F. R., Nehbandani, A., Nendel, C., Purcell, L. C., Qian, B. D., Ruane, A. C., Schoving, C., Silva, E., Smith, W., Soltani, A., Srivastava, A., Vieira, N. A., Slone, S., and Salmeron, M.: Are soybean models ready for climate change food impact assessments?, *European Journal of Agronomy*, 135, 15, 10.1016/j.eja.2022.126482, 2022.
- 760 Lesser, V. M., Rawlings, J. O., Spruill, S. E., and Somerville, M. C.: Ozone effects on agricultural crops: Statistical methodologies and estimated dose-response relationships, *Crop Science*, 30, 148-155, 10.2135/cropsci1990.0011183X003000010033x, 1990.
- Leung, F., Williams, K., Sitch, S., Tai, A. P. K., Wiltshire, A., Gornall, J., Ainsworth, E. A., Arkebauer, T., and Scoby, D.: Calibrating soybean parameters in JULES 5.0 from the US-Ne2/3 FLUXNET sites and the SoyFACE-O-3 experiment, *Geoscientific Model Development*, 13, 6201-6213, 10.5194/gmd-13-6201-2020, 2020.
- 765 Li, T., Hasegawa, T., Yin, X. Y., Zhu, Y., Boote, K., Adam, M., Bregaglio, S., Buis, S., Confalonieri, R., Fumoto, T., Gaydon, D., Marcaida, M., Nakagawa, H., Oriol, P., Ruane, A. C., Ruget, F., Singh, B., Singh, U., Tang, L., Tao, F. L., Wilkens, P., Yoshida, H., Zhang, Z., and Bouman, B.: Uncertainties in predicting rice yield by current crop models under a wide range of climatic conditions, *Global Change Biology*, 21, 1328-1341, 10.1111/gcb.12758, 2015.
- 770 Mills, G., Sharps, K., Simpson, D., Pleijel, H., Frei, M., Burkey, K., Emberson, L., Uddling, J., Broberg, M., Feng, Z. Z., Kobayashi, K., and Agrawal, M.: Closing the global ozone yield gap: Quantification and cobenefits for multistress tolerance, *Global Change Biology*, 24, 4869-4893, 10.1111/gcb.14381, 2018a.
- Mills, G., Sharps, K., Simpson, D., Pleijel, H., Broberg, M., Uddling, J., Jaramillo, F., Davies, W. J., Dentener, F., Van den Berg, M., Agrawal, M., Agrawal, S. B., Ainsworth, E. A., Buker, P., Emberson, L., Feng, Z. Z., Harmens, H., Hayes, F., Kobayashi, K., Paoletti, E., and Van Dingenen, R.: Ozone pollution will compromise efforts to increase global wheat production, *Global Change Biology*, 24, 3560-3574, 10.1111/gcb.14157, 2018b.
- 775 Morris, M. D.: Factorial sampling plans for preliminary computational experiments, *Technometrics*, 33, 161-174, 10.2307/1269043, 1991.
- Mulchi, C. L., Lee, E., Tuthill, K., and Olinick, E. V.: Influence of ozone stress on growth-processes, yields and grain quality characteristics among soybean cultivars, *Environmental Pollution*, 53, 151-169, 10.1016/0269-7491(88)90031-0, 1988.
- 780 NRCS, S. S. S.: Natural Resources Conservation Service, United States Department of Agriculture. Web Soil Survey, 2023.
- Osborne, S. A., Mills, G., Hayes, F., Ainsworth, E. A., Buker, P., and Emberson, L.: Has the sensitivity of soybean cultivars to ozone pollution increased with time? An analysis of published dose-response data, *Global Change Biology*, 22, 3097-3111, 10.1111/gcb.13318, 2016.
- 785 R Core Team: R: a language and environment for statistical computing, 2023.
- Ritchie, J. T., Alocilja, E. C., Singh, U., and Uehara, G.: IBSNAT and the CERES-RICE model, in: *Weather and Rice, Proceedings of the International Workshop on The Impact of Weather Parameters on Growth and Yield of Rice*, IRRI, Philippines, 271-283, 1987.
- 790 Rosenzweig, C., Jones, J. W., Hatfield, J. L., Ruane, A. C., Boote, K. J., Thorburne, P., Antle, J. M., Nelson, G. C., Porter, C., Janssen, S., Asseng, S., Basso, B., Ewert, F., Wallach, D., Baigorria, G., and Winter, J. M.: The Agricultural Model Intercomparison and Improvement Project (AgMIP): Protocols and pilot studies, *Agricultural and Forest Meteorology*, 170, 166-182, 10.1016/j.agrformet.2012.09.011, 2013.
- 795 Sampedro, J., Waldhoff, S. T., Van de Ven, D. J., Pardo, G., Van Dingenen, R., Arto, I., del Prado, A., and Sanz, M. J.: Future impacts of ozone driven damages on agricultural systems, *Atmospheric Environment*, 231, 11, 10.1016/j.atmosenv.2020.117538, 2020.

Schauberger, B., Rolinski, S., Schaphoff, S., and Muller, C.: Global historical soybean and wheat yield loss estimates from ozone pollution considering water and temperature as modifying effects, *Agricultural and Forest Meteorology*, 265, 1-15, 10.1016/j.agrformet.2018.11.004, 2019.

800 Schiferl, L. D. and Heald, C. L.: Particulate matter air pollution may offset ozone damage to global crop production, *Atmospheric Chemistry and Physics*, 18, 5953-5966, 10.5194/acp-18-5953-2018, 2018.

Simpson, D., Arneth, A., Mills, G., Solberg, S., and Uddling, J.: Ozone - the persistent menace: interactions with the N cycle and climate change, *Current Opinion in Environmental Sustainability*, 9-10, 9-19, 10.1016/j.cosust.2014.07.008, 2014.

805 Szopa, S., Naik, V., Adhikary, B., Artaxo, P., Berntsen, T., Collins, W. D., Fuzzi, S., Gallardo, L., Kiendler-Scharr, A., Klimont, Z., Liao, H., Unger, N., and Zanis, P.: 2021: Short-Lived Climate Forcers, in: *Climate Change 2021: The Physical Science Basis. Contribution of Working Group I to the Sixth Assessment Report of the Intergovernmental Panel on Climate Change*, edited by: Masson-Delmotte, V., Zhai, P., Pirani, A., Connors, S. L., Péan, C., Berger, S., Caud, N., Chen, Y., Goldfarb, L., Gomis, M. I., Huang, M., Leitzell, K., Lonnoy, E., Matthews, J. B. R., Maycock, T. K., Waterfield, T., Yelekçi, O., Yu, R., and Zhou, B., Cambridge University Press, Cambridge, United Kingdom and New York, NY, USA, 817-922, 10.1017/9781009157896.008, 2021.

810 Tai, A. P. K., Sadiq, M., Pang, J. Y. S., Yung, D. H. Y., and Feng, Z. Z.: Impacts of Surface Ozone Pollution on Global Crop Yields: Comparing Different Ozone Exposure Metrics and Incorporating Co-effects of CO₂, *Frontiers in Sustainable Food Systems*, 5, 18, 10.3389/fsufs.2021.534616, 2021.

815 Toreti, A., Deryng, D., Tubiello, F. N., Muller, C., Kimball, B. A., Moser, G., Boote, K., Asseng, S., Pugh, T. A. M., Vanuytrecht, E., Pleijel, H., Webber, H., Durand, J. L., Dentener, F., Ceglar, A., Wang, X. H., Badeck, F., Lecerf, R., Wall, G. W., van den Berg, M., Hoegy, P., Lopez-Lozano, R., Zampieri, M., Galmarini, S., O'Leary, G. J., Manderscheid, R., Contreras, E. M., and Rosenzweig, C.: Narrowing uncertainties in the effects of elevated CO₂ on crops, *Nature Food*, 1, 775-782, 10.1038/s43016-020-00195-4, 2020.

820 USDA NASS: Field crops usual planting and harvest dates (October 2010), 2010.

Wang, X. P. and Mauzerall, D. L.: Characterizing distributions of surface ozone and its impact on grain production in China, Japan and South Korea: 1990 and 2020, *Atmospheric Environment*, 38, 4383-4402, 10.1016/j.atmosenv.2004.03.0367, 2004.

Wickham, H.: *ggplot2: elegant graphics for data analysis*, 2016.

825 Wickham, H., François, R., Henry, L., Müller, K., and Vaughan, D.: *dplyr: a grammar of data manipulation*. R package version 1.1.2, 2023.

Wilkerson, G. G., Jones, J. W., Boote, K. J., Ingram, K. T., and Mishoe, J. W.: Modeling soybean growth for crop management, *Transactions of the Asae*, 26, 63-73, 1983.

830 Xia, L. L., Lam, S. K., Kiese, R., Chen, D. L., Luo, Y. Q., van Groenigen, K. J., Ainsworth, E. A., Chen, J., Liu, S. W., Ma, L., Zhu, Y. H., and Butterbach-Bahl, K.: Elevated CO₂ negates O₃ impacts on terrestrial carbon and nitrogen cycles, *One Earth*, 4, 1752-1763, 10.1016/j.oneear.2021.11.009, 2021.

Zhang, Y. Z. and Wang, Y. H.: Climate-driven ground-level ozone extreme in the fall over the Southeast United States, *Proceedings of the National Academy of Sciences of the United States of America*, 113, 10025-10030, 10.1073/pnas.1602563113, 2016.

835